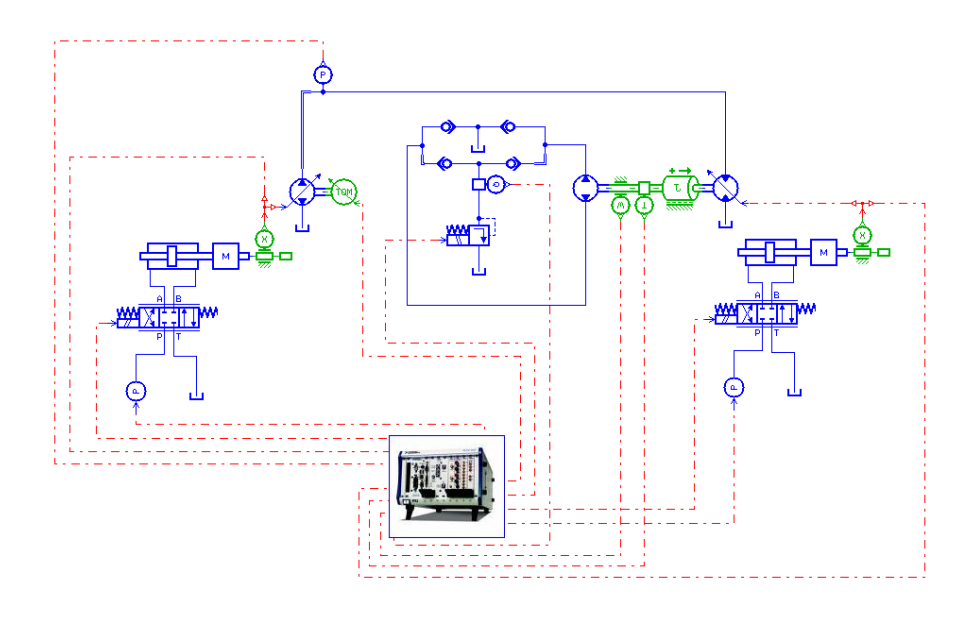


Doctoral thesis name:

Theoretical and experimental contributions on optimizing the dynamic parameters of multifunctional motor trucks by using hydrostatic transmissions

RESEARCH REPORT NO. 3

Numerical simulation, mathematical modeling and experimentation of hydraulic transmissions specific to self-propelled machines



Field of doctoral studies: Mechanical Engineering Specialization: Technical Mechanics and Vibrations

Doctoral Supervisor: Prof. PhD Eng. Cristian Pavel

Doctoral Student: Dipl. eng. Chiriță Alexandru-Polifron



Table of Contents

1.	Introduction 1
2.	Structure of the hydraulic transmission with mixed control
	2.1. Conclusions on building the hydraulic transmission with mixed control 5
	2.2. Numerical simulation and experimental identification of the hydraulic servomechanism controlling the capacity of the RKP-D type MOOG pump 5
	2.3. Numerical simulation of the RKP-D type MOOG pump7
	2.4. Testing of the RKP-D type MOOG servo pump 8
	2.4.1. Stationary testing8
	2.4.2. Dynamic testing8
	2.5. Conclusions on numerical simulation and experimental identification of the RKP-D type MOOG pump capacity control device9
	Control of hydrostatic transmissions by virtual instrumentation technique 10
	3.1. Considerations regarding modern methods of simulation and testing of hydraulic drive systems10
	3.2. Control model of hydrostatic transmission with mixed control11
	3.3. Mathematical model of mixed control hydrostatic transmission
	3.4. Detailed model of the simulation network and virtual interface of the control model14
	3.5. Dynamic characteristics of mixed control hydrostatic transmission, achieved by numerical simulation
	3.6. Experimental validation of the hydrostatic transmission control model 16
	3.7. Conclusions on modeling, simulation and testing of mixed control hydraulic transmission
4.	Energy and functional advantages of adjustable hydraulic transmissions
	4.1. Considerations regarding the energy advantages of adjustable hydraulic transmissions
	4.2. Basic model and numerical simulation network of primary control hydraulic transmission
	4.3. Energy efficiency analysis of hydraulic transmissions with fixed or adjustable capacity pumps23
	4.4. Conclusions on the energy efficiency of hydraulic transmissions with fixed or adjustable capacity pumps25
5	Virtual tests on secondary control hydraulic transmissions



5.1. Secondary control hydraulic transmission with fixed capacity pump at capacity motor	
5.1.1. Mathematical modeling of hydraulic transmission	26
5.1.2. Numerical simulation of hydraulic transmission	29
5.2. Secondary control hydraulic transmission with adjustable capacity pur capacity motor and PID compensator in the speed control loop	•
5.3. Secondary control hydraulic transmission with adjustable capacity equipped with pressure controller and variable capacity motor	, , , ,
5.4. Conclusions on the secondary control of hydraulic transmissions	43
RIRI IOGRAPHY	45



1. Introduction

Three types of hydraulic transmission control are mentioned in the literature:

- -primary control, in which the positive displacement machine (the pump) in the primary side of the transmission has an adjustable capacity, while the one (the motor) in the secondary side, fed at a constant flow rate, has a fixed capacity;
- -secondary control, in which the positive displacement machine in the primary side of the transmission has a fixed capacity, while the one in the secondary side, fed at a constant pressure rate, has an adjustable capacity;
- **-mixed control**, in which the positive displacement machines in the primary and secondary sides of the transmission have adjustable capacities.



2. Structure of the hydraulic transmission with mixed control

The experimental model of hydraulic transmission with mixed control comprises in the primary side a MOOG servo pump, type RKP-D, with 9 radial pistons, which has a capacity of $V_p=32 \, \mathrm{cm}^3/\mathrm{rev}$ and rotational speed of n=1450 rpm. With an adjustable control signal of 0 ... 10V, the servo pump can supply a variable flow rate of 0...46 l/min. Fig. 1 shows a cross section view of the servo pump, and fig. 2 – the basic hydraulic schematic diagram.

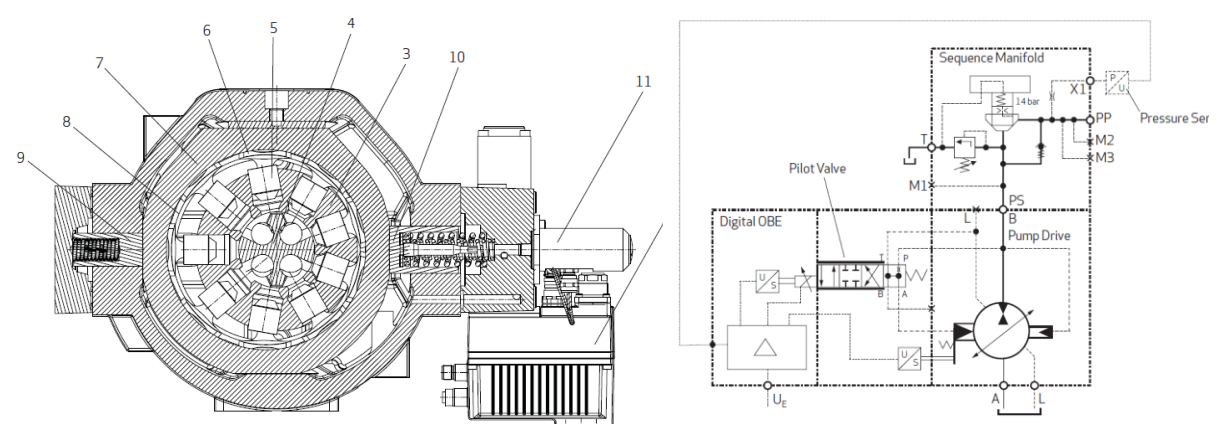


Fig. 1- Cross section view of the RKP-D type MOOG servo pump.

Fig. 2- Basic hydraulic schematic diagram for the RKP-D servo pump.

The RKP-D type MOOG servo pump (fig. 1) has 9 radial pistons (item 5), mounted in a block of cylinders (item 3). During rotation of the block of cylinders, by its drive by the pump shaft, the pistons generate chambers of variable capacity, having a linear block movement, only if the pump capacity control ring (item 7) is eccentric with respect to the pump shaft. The size of this eccentricity determines the stroke of the pistons and, implicitly, the capacity of the pump. By means of a distribution system, located in the shaft of the block of cylinders, each piston of the pump is connected, alternately, to each rotation of the block, on ½ rev. at the pump suction and on ½ rev. at the pump discharge.

Automatic drive and control of the control ring is performed by means of a hydraulic position control servomechanism, consisting of: two pistons of different diameters (item 9 and item 10), a servovalve (item 12), two position transducers, the first placed on the control ring and the second - on the servovalve spool, a pressure transducer, located on the pump discharge and an electronic control unit (item 11).

The modular structure of the RKP-D servo pump (fig. 2) comprises four modules: **electronic control unit**; **capacity control servomechanism**; **pump**; **Sequence Manifold module**, which does not allow the pressure on the pump discharge to fall below the control ring pressure (14 bar).

The RKP-D type MOOG servo pump, according to fig. 3, works with closed circuit - digital or analog - control. Through experimental tests, it is possible to intervene in the MOOG CONFIGURATION SOFTWARE in order to change the values of the factory default parameters, in accordance with the parameters of the hydraulic drive system in which it is to be mounted. It can be used in all three types of hydraulic transmissions based on automatic control of the capacity of rotary positive displacement machines:

for hydraulic transmission (HT) with primary control, the RKP-D type MOOG servo pump with flow loop control ($U_E=Q$) in the primary side and a constant capacity rotary hydraulic motor in the secondary side can be used; for HT with secondary control, the RKP-D type MOOG servo pump with pressure loop control ($U_E=P$) in the primary side and a rotary hydraulic servomotor (with adjustable capacity) in the secondary side can be used; for HT with mixed control, the RKP-D type MOOG servo pump with flow loop control ($U_E=Q$) in the primary side and a rotary hydraulic servomotor (with adjustable capacity) in the secondary side can be used.



Fig. 3- RKP-D type MOOG servo pump in the primary side of the hydrostatic transmission.

The EP2 type BOSCH hydraulic servomotor (fig. 4) in the secondary side of the hydrostatic transmission has minimal - mechanically limited - capacity, $V_{m\ min}$ = 7 cm³/rev, for a control signal of 200 mA, maximum capacity of $V_{m\ max}$ = 28 cm³/rev, for a control signal of 800 mA, and it is powered at 24 V DC. According to its basic schematic diagram (fig. 5), this servomotor with integrated electronics can be controlled so that when the load increases / decreases, the capacity decreases / increases automatically, keeping the speed relatively constant, within certain limits. This type of control will be used for secondary or mixed control of hydrostatic transmissions.



Fig.4- EP2 type Bosch hydraulic servomotor.

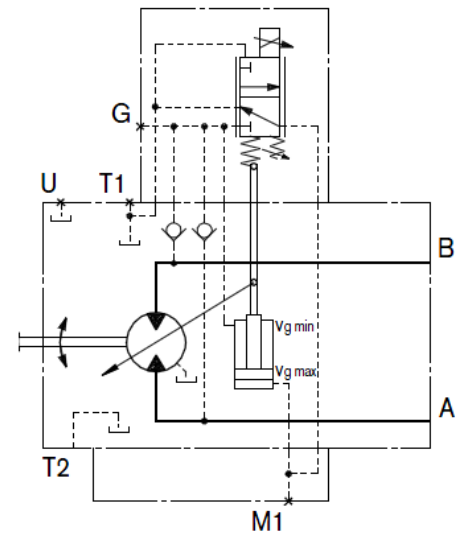


Fig.5 Hydraulic basic diagram of EP2 type Bosch hydraulic servomotor.

The EP2 type BOSCH hydraulic servomotor in the secondary side of the mixed control hydrostatic transmission is coupled to a hydraulic load simulation device (fig. 6). This hydraulic servomotor is powered by the MOOG servo pump in the primary side of the mixed control hydrostatic transmission (fig. 7). The fixed displacement bent-axis axial piston pump, simulating the load for the Bosch servomotor, is supplied from the tank in the secondary side of the transmission by means of a pre-supply pump and a 4-way valve bridge.



Fig.6- EP2 type Bosch servomotor in the secondary side of the hydrostatic transmission (right), coupled to the hydraulic load simulation device.



Fig.7- Power supply to the load pump and Bosch servomotor.

The load simulation module for servomotor, with DSSq-SH code hydraulic basic diagram, comprises three main subassemblies: hydraulic pressure and flow control devices, oil tank, and load simulation device for servomotor.

The hydraulic pressure and flow control devices are located on the oil tank cover. They include one REXROTH Dn10 proportional pressure valve, four Dn16 check valves, one Dn 8 ball valve, two Dn16 ball valves, three manometers, two pressure transducers.

The oil tank it is equipped with a filling and ventilating filter and an oil-level indicator.

The load simulation device for servomotor comprises a closed frame type support, on which two rotary positive displacement machines - a pump and a motor, whose shafts are mechanically coupled - are mounted. A torque transducer and a wheel with 60 equal teeth for the rotation transducer are mounted on the couplings.

Operation of the load simulation device for servomotor

The rotary hydraulic motor that is tested at variable load, namely the EP2 type BOSCH servomotor, is mounted on the device. It can be used as a fixed capacity motor or a variable capacity servomotor, adjustable by a hydraulic position control servomechanism. The variable load is achieved with the help of the proportional valve mounted on the discharge of the fixed capacity pump, mechanically coupled to the hydraulic motor. The fixed capacity pump is supplied from the tank, through the bridge of the four check valves and the pre-supply pump, and the Bosch hydraulic motor from the pumping unit of the primary side of the transmission (SPDM-0-SH code hydraulic diagram).

With the load simulation device, which is the secondary side of the mixed control hydrostatic transmission (DSSq-SH code hydraulic diagram) and the pumping unit containing the RKP-D type MOOG servo pump (SPDM-0-SH code hydraulic



diagram), three types of hydraulic drive systems (HDS) can be tested, based on automatic control of rotary positive displacement machines, advantageous in terms of energy:

- a) HDS with control in the primary side, in which the pump within the additional pumping unit is used as an adjustable capacity pump with hydraulic capacity control servomechanism, and the Bosch servomotor within the load simulation device operates as a fixed capacity rotary hydraulic motor;
- b) **HDS with control in the secondary side**, in which the MOOG servo pump in the primary side is used as a fixed capacity pump, and the Bosch servomotor within the load simulation device is used as an adjustable capacity rotary motor with hydraulic capacity control servomechanism;
- c) HDS with control in the secondary and primary sides (mixed control), in which adjustable positive displacement machines, equipped with hydraulic capacity control servomechanisms, are used in both primary and secondary sides.

2.1. Conclusions on building the hydraulic transmission with mixed control

The mixed control hydraulic transmission has been made in modular construction, which is based, in the primary and secondary sides, on: two adjustable positive displacement machines with suitable control electronics; a hydraulic device for simulating the load of the positive displacement machine in the secondary side; an electrical panel and a power supply; two oil tanks; pressure, speed, flow and torque transducers; hydraulic pressure distribution and control equipment; accessories for fastening / connecting mechanical and hydraulic components.

Using a data acquisition board, a signal generator, a PXI-NATIONAL INSTRUMENTS block and the specialized LabVIEW or Test Point software, on this hydraulic drive system one can experimentally identify specific characteristics of the primary, secondary or mixed control of hydraulic transmissions.

The possibility of experimental identification of the functional characteristics specific to the three types of control, raised on the same type of hydraulic installation, is a major economic advantage.

The adaptability of this hydraulic transmission to experimentally simulate each of the three types of control is due to the ability of positive displacement machines in the primary and secondary sides to operate in two modes: with fixed capacity or adjustable capacity.

2.2. Numerical simulation and experimental identification of the hydraulic servomechanism controlling the capacity of the RKP-D type MOOG pump

From the point of view of the theory of automated systems, the RKP-D type MOOG radial piston pump capacity control servomechanism is a position control hydraulic servomechanism. The AMESim simulation model (fig. 8) comprises: a 4/3 proportional directional control valve, closed center type; a pressurized oil supply unit; a tank; a position transducer; a compensator; a linear hydraulic motor with inertial load and viscous friction; a signal generator.

To determine the static and dynamic characteristics, the system was excited with triangular, control step and sine signals. The frequency of the ramp signal has

been chosen low enough to generate a quasi-static regime. The following characteristics were obtained after simulation and testing: the response of the servomechanism over time to the excitation signals (fig. 9, fig. 10, fig. 11, fig. 12) and the stationary characteristic (fig. 13).

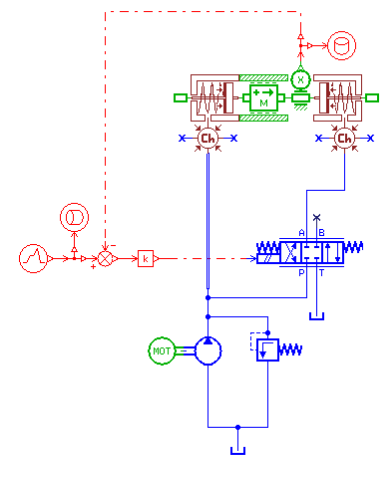


Fig.8- Simulation network of the RKP-D pump capacity control servomechanism.

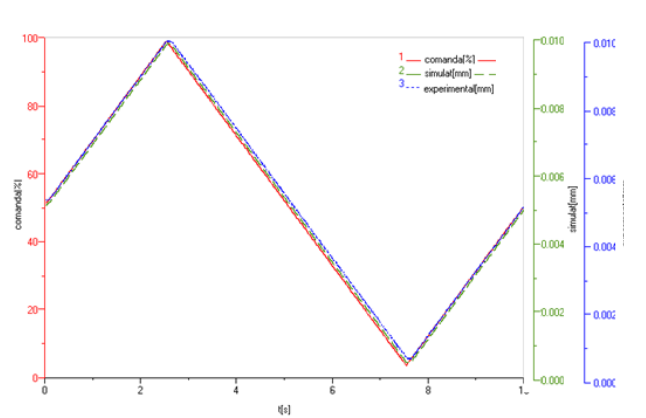


Fig. 9- System response to triangular signal, f=0.1 Hz (control-in red; simulated-in green; experimental-in blue).

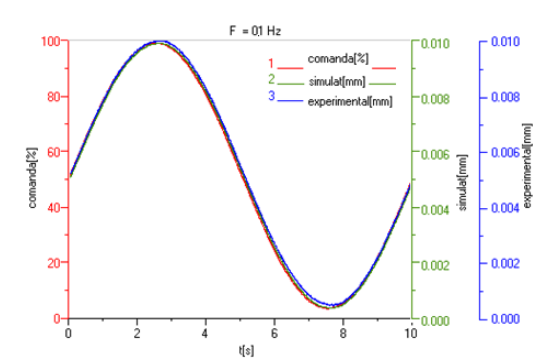


Fig. 10- System response to sine signal, f=0.1 Hz (control-in red; simulated-in green; experimental-in blue).

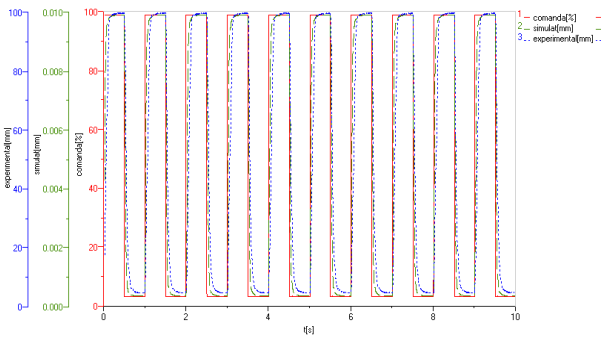


Fig. 11- System response to rectangular signal, f=1 Hz (control-in red; simulated-in green; experimental-in blue).

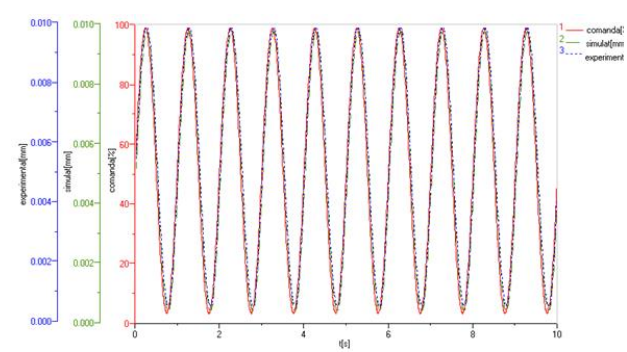


Fig. 12- System response to sine signal, f=1 Hz (control-in red; simulated-in green; experimental-in blue).

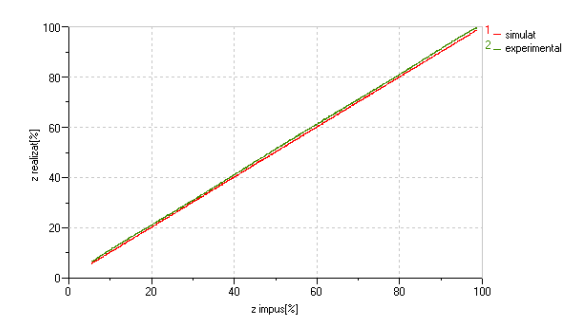


Fig. 13- Stationary displacement characteristic: Zachieved =f(Zrequired), f =0.05Hz (simulated-in red; experimental-in green).



2.3. Numerical simulation of the RKP-D type MOOG pump

The AMESim simulation network model (fig. 14) comprises: the RKP-D type MOOG pump capacity control servomechanism (top right corner, see fig. 8); the 9 radial pump pistons, each with a piston stroke simulation submodel, depending on its reference angular position relative to the eccentricity of the control ring (see detail in fig. 15); and one distribution submodel for each of the piston suction and discharge phases (see detail in fig. 16). Fig. 17 and fig. 18 show the flow characteristics for each radial piston and for the pump assembly.

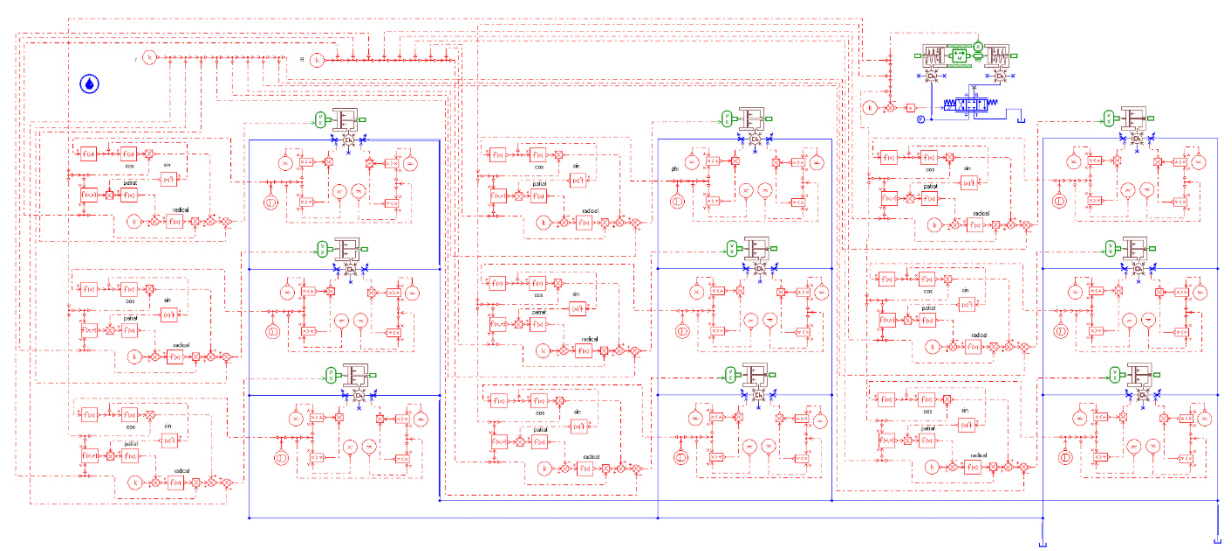


Fig. 14- The AMESim simulation network for the RKP-D type MOOG pump.

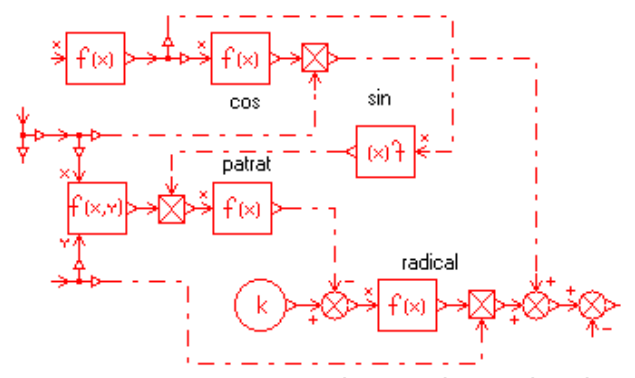


Fig. 15- Pump piston stroke simulation detail.

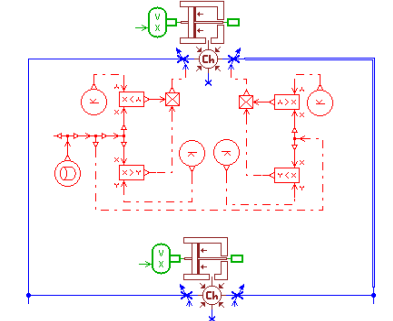


Fig. 16- Pump piston distribution simulation detail.

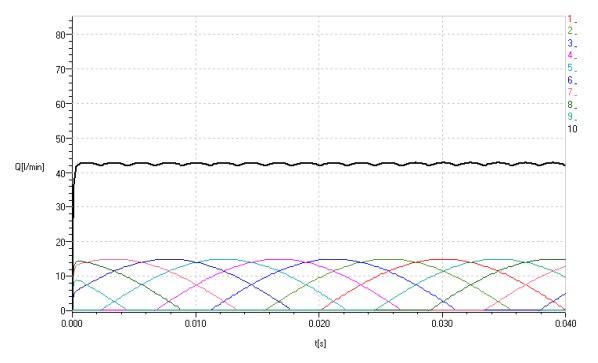


Fig. 17- Flow characteristic Q=f(t) for the RKP-D pump (no load).

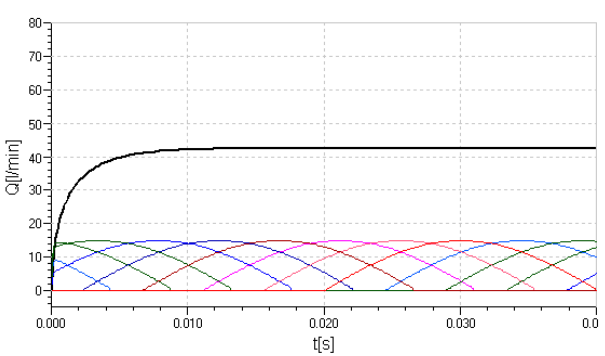


Fig. 18- Flow characteristic Q=f(t) for the RKP-D pump (12-bar load)



2.4. Testing of the RKP-D type MOOG servo pump

The acquisition of experimental data for servo pump testing has been performed using the LabVIEW software and the DAQ NI PXI-1031 programmable logic controller (PLC).

2.4.1. Stationary testing

Fig. 19 shows the servo pump response (achieved flow rate) to a control ramp signal, with maximum amplitude and frequency of 0.1 Hz, and fig. 20 shows the dependence of the controlled parameter (pump flow rate) on the control parameter (eccentricity of the control ring).

Hysteresis is found - on the x^n -axis abscissa (control parameter) and on the x^n -axis ordinate (controlled parameter) - to be very small.

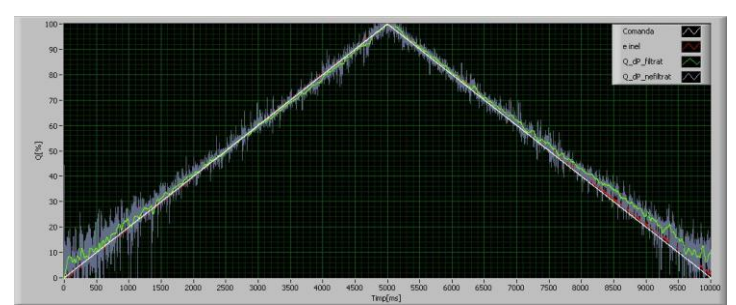


Fig. 19- Response to ramp signal with A=100% and f=0.1Hz /in white-control signal /in red-position of control ring / in blue-achieved flow rate / in green-filtered flow rate signal.

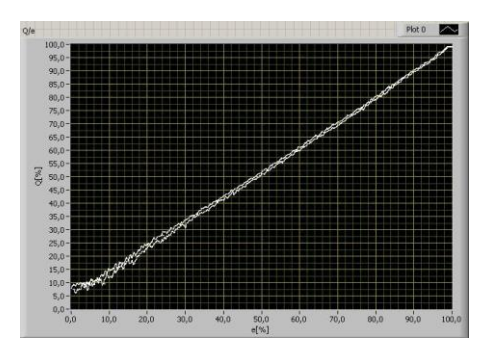


Fig. 20- Flow rate - control ring eccentricity dependence.

2.4.2. Dynamic testing

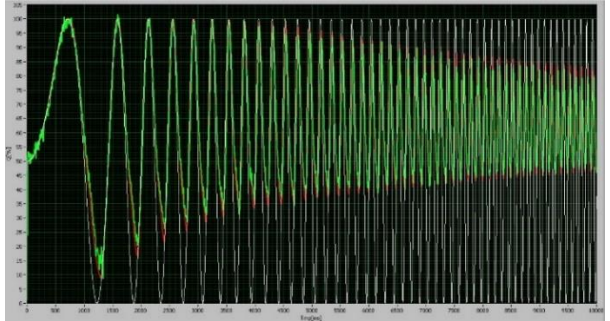


Fig.21- Response to sine signal with A=100%, f=0..20Hz / in white-control signal / in green-Qachieved / in red-position of control ring.

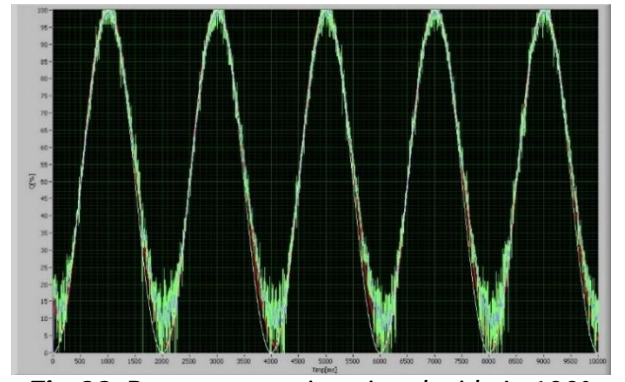


Fig.22- Response to sine signal with A=100% and f=0.5Hz / in white-control signal / in redposition of control ring / in green—achieved flow rate.

For dynamic testing (fig. 21...fig. 24) a flow transducer was used, consisting of a diaphragm and two pressure transducers, much more sensitive than the turbine transducer.



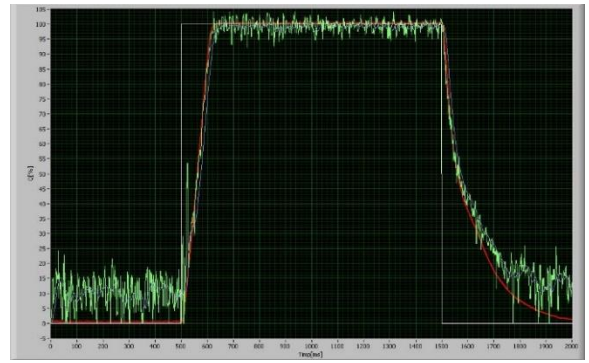


Fig.23- Response to rectangular signal with A=100% and f=0.5Hz / in white-control signal / in red-position of control ring / in green—achieved flow rate / in blue—filtered diaphragm flow rate signal.

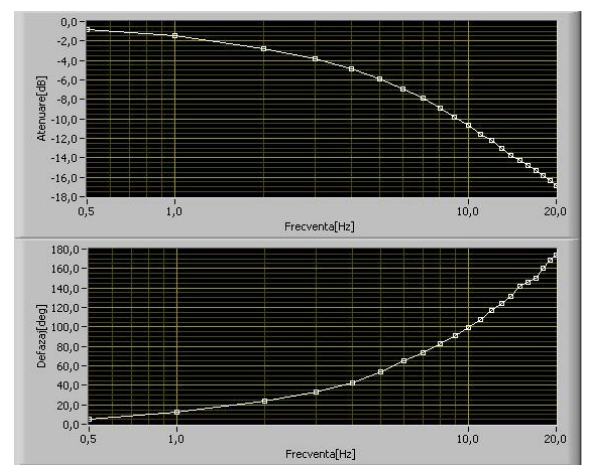


Fig.24- BODE diagrams: Cutting frequency (at -3dB) = 2.2Hz.

2.5. Conclusions on numerical simulation and experimental identification of the RKP-D type MOOG pump capacity control device

- The results of the experimental tests performed on the RKP-D type MOOG pump capacity control device have validated the simulation model of the device, made in the AMESim software;
- The results of the experimental tests performed on the RKP-D type MOOG pump equipped with capacity control device have validated the simulation model of the pump, made in the AMESim software;
- The RKP-D type MOOG pump simulation model has been integrated as a supercomponent in the simulation models of hydrostatic transmissions with primary, secondary or mixed control.



3. Control of hydrostatic transmissions by virtual instrumentation technique

3.1. Considerations regarding modern methods of simulation and testing of hydraulic drive systems

Electrohydraulic control systems are complex systems, in which both phenomena associated with the flow of fluids, in the field of hydraulic positive displacement transmissions, and phenomena specific to automatic control processes intervene. Due to the complexity of these phenomena, determining the optimal solutions in the design and implementation of electrohydraulic control systems is iterative, usually using dedicated languages.

Benefiting from process identification methods and the power of numerical computing equipment, researchers and designers can shorten the development period of applications in various fields, by generating solutions as close to reality as possible, right from the design phase.

For open circuit hydrostatic transmission with mixed control, with RKP-D type MOOG servo pump in its primary side and EP2 type Bosch servomotor in its secondary side, a hybrid modeling / simulation / testing solution is presented.

Starting from a well-known mathematical model, that of a hydrostatic transmission, using two different modeling / simulation environments, AMESim and LabVIEW, a system control model has been created, optimized and experimentally validated.

The latest trends in modeling and simulation of dynamic systems aim at new concepts, such as cosimulation and real-time simulation.

The concept of real-time simulation of dynamical systems allows the simultaneous existence of both a part of a mathematical model and a part of a physical model, thus obtaining a decrease in the degree of inaccuracy caused by certain phenomena neglected in the mathematical model.

Cosimulation involves the simultaneous use of the resources of several modeling / simulation environments, with the possibility to benefit from the maximum performance of each environment.

The concepts of cosimulation and real-time numerical simulation are not newly developed concepts. Due to their potential and rapid evolution over time, numerical computing systems have begun to enter the industrial control and adjustment area relatively recently since their emergence. However, due to the specific languages used by these machines, their control and programming has been for a long time the prerogative of computer specialists. The obvious need for use by a much wider range of users, especially by those in scientific fields who make complex mathematical models, has led to the evolution of specialized interpreters, i.e. easy languages for control / programming of computing equipment.

For the mixed control transmission developed an actual example of a numerical cosimulation network is presented, based on two software programs: AMESim and LabVIEW. By using the AMESim software program, the hydrostatic transmission model has been created, and the analysis of the data obtained from simulations in AMESim has been performed by using virtual instrumentation, through the LabVIEW software program.



Simultaneous use of the two simulation / programming environments, AMESim and LabVIEW, can result in the development of advanced modeling / simulation networks of electrohydraulic systems.

Modern methods of experimentation in the field of hydraulic and pneumatic drive systems involve the existence of at least one numerical computing equipment. The need to use electrohydraulic converters for controlling and adjusting various physical parameters, such as force and displacement, along with the exponential development of digital electronics, confirms this. Digital equipment can be found in sensors and transducers, digital displays, electronic servo amplifiers (compensators) or process computers.

Sensors and transducers with electronic communication interface, as well as control systems (proportional electrohydraulic directional control valves, hydraulic or pneumatic servo pumps /servomotors, etc.) with analog / digital control ports and electronic control blocks can not miss from the infrastructure of any modern laboratory of electrohydraulic drives.

By a "smart" combination of these devices, various installations, equipment, benches with specific functionalities can be created. Coupling industrial computers to these systems enables a flexible "manipulation" of the functionalities of the mentioned systems. The possibility to "load" the numerical computing systems with "virtual models" of systems, developed with the help of advanced modeling languages, further increases their flexibility.

Three types of control are known for hydrostatic transmissions:

- -primary control, in which the positive displacement machine (the pump) in the primary side of the transmission has an adjustable capacity, while the one (the motor) in the secondary side, fed at a constant flow rate, has a fixed capacity;
- -secondary control, in which the positive displacement machine in the primary side of the transmission has a fixed capacity, while the one in the secondary side, fed at a constant pressure rate, has an adjustable capacity;
- **-mixed control**, in which the positive displacement machines in the primary and secondary sides of the transmission have adjustable capacities.

In terms of functional performance and energy saving, hydrostatic transmissions based on secondary control have advantages over those based on primary control. However, they raise some difficulties, especially in the case of long lines, with several consumers, related to the influence of the variation of the load of some consumers on the variation of the load of the other consumers.

3.2. Control model of hydrostatic transmission with mixed control

The analyzed hydrostatic transmission, with mixed control, with a single consumer type rotary, adjustable positive displacement motor, according to fig. 25, comprises:

- in the primary side: MOOG servo pump, item 1, with radial pistons and integrated electronics, with three control loops, namely (1) in flow, (2) in pressure, and (3) in flow and pressure; electric motor for driving the servo pump, constant speed, item 2; pressure limiting valve, item 3; flow transducer, item 4; pressure transducer, item 5.
- in the secondary side: BOSCH servomotor, item 7, with axial pistons, bent-axis and integrated electronics; torque transducer, item 8; speed transducer, item 9; axial piston

pump, bent-axis, fixed capacity, item 10, to simulate the load of the hydraulic servomotor; two pressure transducers, item 11 and item 13; four check valves, item 12, mounted on the suction / discharge of the load pump; electrically operated pressure control valve, item 14, to control the load of the hydraulic servomotor.

- a PXI-NATIONAL INSTRUMENTS **block**, item 6, which provides the virtual interface for the process of controlling the capacity of adjustable positive displacement machines (LabVIEW / PXI).

The hydrostatic transmission control model ensures the automatic, successive change of the capacity of the two adjustable positive displacement machines, depending on the speed variation at the hydraulic motor shaft.

There is a programmable threshold of the hydraulic motor speed up to which increasing its speed requires the control system to control the pump capacity in the direction of increasing it, simultaneously with maintaining the motor at maximum capacity, and exceeding this threshold requires the control system to control the motor capacity in the direction of decreasing it, simultaneously with maintaining the pump capacity at the value corresponding to the moment the speed threshold is reached.

In order to optimize the control model of the analyzed hydrostatic transmission, the following steps have been iteratively followed:

a) A basic model of the mixed control hydrostatic transmission has been developed (fig. 25);

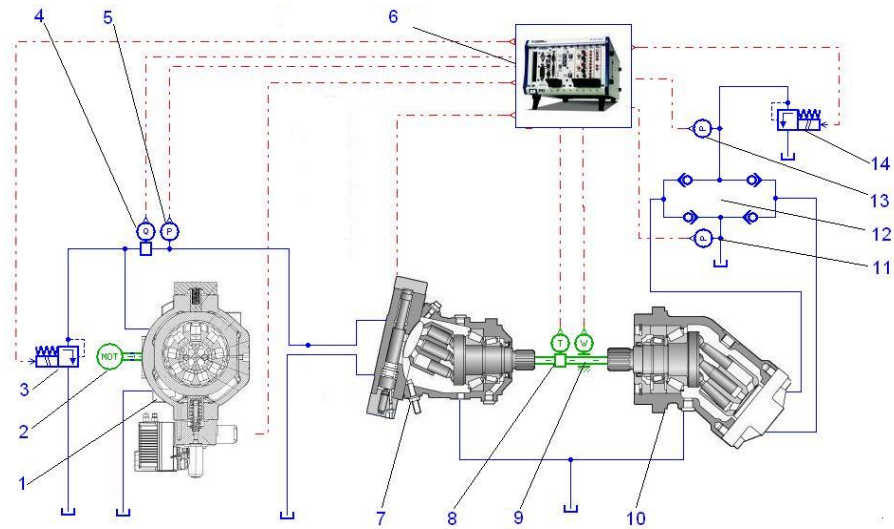


Fig.25- Basic model of the mixed control hydrostatic transmission.

- b) The mathematical model of the mixed control hydraulic transmission has been determined;
- c) The AMESim simulation model of the transmission has been created, see fig. 26;
- d) The virtual interface of the control process has been created in LabVIEW, see fig. 27, which has been connected to the simulation network, developed in AMESim;
- e) The dynamic behavior of the hydrostatic transmission at speed step signals prescribed to the hydraulic motor has been simulated, which involves control signals for adjusting the capacity of the hydraulic pump / motor.
- f) The hydrostatic transmission control model has been experimentally validated, by disconnecting the LabVIEW / PXI virtual interface from the AMESim simulation model, followed by the coupling of this interface to the physical, laboratory model, raising the

experimental dynamic characteristics and comparing them with those resulting from simulations.

3.3. Mathematical model of mixed control hydrostatic transmission

The mathematical model of the hydraulic system in fig. 26 is characterized by the following equations:

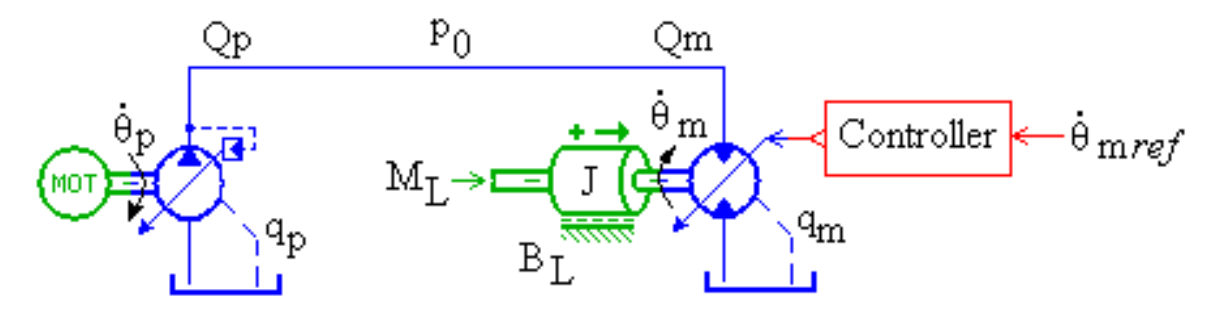


Fig.26- Schematic diagram of open circuit hydrostatic transmission.

Pump flow conservation equation:

$$Q_{p} = V_{p}\theta_{p}^{'} - C_{pi}(P_{0} - P_{tank}) - C_{pe}P_{0}$$
 (1)

$$V_{p} = \frac{\alpha_{p}V_{pmax}}{2\pi}$$
 (2)

$$q_{p} = C_{pe}(P_{0} - P_{tank})$$
 (3)

Pressure line flow conservation equation:

$$Q_{p} - Q_{m} = \frac{dP_{0}}{dt} \left(k_{e} + \frac{V_{c}}{E} \right)$$
 (4)

Hydraulic motor flow conservation equation:

$$Q_{m} = V_{m}\theta'_{m} + C_{mi}(P_{0} - P_{tank}) + C_{me}P_{0}$$
 (5)
$$V_{m} = \frac{\alpha_{m}v_{mmax}}{2\pi}$$
 (6)
$$q_{m} = C_{me}(P_{0} - P_{tank})$$
 (7)

Equilibrium of moments at the level of the hydraulic motor equation:

$$J\frac{d^{2}\theta_{m}}{dt^{2}} + B_{L}\frac{d\theta_{m}}{dt} = V_{m}(P_{0} - P_{tank}) - B_{m}\frac{d\theta_{m}}{dt}M_{L}$$
 (8)

The meaning of the terms in equations (1) ... (8) is as follows:

 α_p – pump control angle;

 $\alpha_{\rm m}$ – motor control angle;

V_p – adjustable pump geometric displacement volume;

V_m - adjustable motor geometric displacement volume;

 θ_{p} – angular pump drive speed;

 $\theta_{m}^{'}$ – angular motor speed;

q_p – external flow loss from pump;

qm - external flow loss from motor;

Q_p – pump outlet flow;



Q_m - motor intlet flow;

P₀ – working circuit pressure;

M_L − load moment (disturbance);

B_L - load damping coefficient;

B_m – friction due to viscosity coefficient;

J - moment of inertia of motor driven mass;

 θ'_{mref} – angular speed imposed on the engine;

C_{pi} – pump internal flow loss coefficient;

C_{mi} – motor internal flow loss coefficient;

C_{pe} – pump external flow loss coefficient;

C_{me} - motor external flow loss coefficient;

ke - coefficient of elasticity for pipes;

V_c – pump-motor pipe capacity;

E - working fluid modulus of elasticity.

The simulation network parameters are:

 $n_{electric motor}$ =1450 rpm; $V_{p max}$ = 32 cm³/rev;

 $V_{m max} = 28 cm^3/rev; V_{p load} = 125 cm^3/rev;$

E = 14000 bar; $J = 0.01 \text{ Kgm}^2$; $B_m = 0.08 \text{ Nm/(rev/min)}$.

3.4. Detailed model of the simulation network and virtual interface of the control model

The detailed simulation network model, see fig. 27, uses components of AMESim libraries and comprises: the adjustable pump in the hydraulic transmission primary side, which supplies the hydraulic motor in the secondary side of the transmission at constant pressure; the hydraulic servomechanism for controlling the capacity of this pump, with its pressure source; the electric motor driving the pump in the primary side; the rotary, adjustable hydraulic motor in the secondary side of the transmission; the hydraulic servomechanism for controlling the capacity of this motor, with its pressure source; fixed capacity, bidirectional pump for simulating the load of the hydraulic motor; four check valves, which ensure the suction / discharge of the fixed capacity pump; a pressure control valve with proportional electrical control, which adjusts the hydraulic motor load value; two position transducers; three pressure transducers; a flow transducer; a torque transducer; a speed transducer; an oil tank; a PXI module.

The virtual interface of the mixed control hydrostatic transmission control model, according to fig. 28, enables:

- prescribing the supply pressure of the two hydraulic position control servomechanisms, which adjusts the capacities of the two adjustable positive displacement machines;
- prescribing the load value of the rotary hydraulic motor in the secondary side of the transmission;
- prescribing the value of the pressure on the discharge circuit of the pump in the primary side of the transmission and maintaining this value automatically, by changing the pump capacity according to the direction and size of the controlled pressure variation;



- prescribing the speed of the rotary hydraulic motor in the secondary side of the transmission and maintaining this value automatically, by changing the capacity of the hydraulic motor in the secondary side, when its speed tends to increase or decrease, depending on the variation of the load on the shaft.

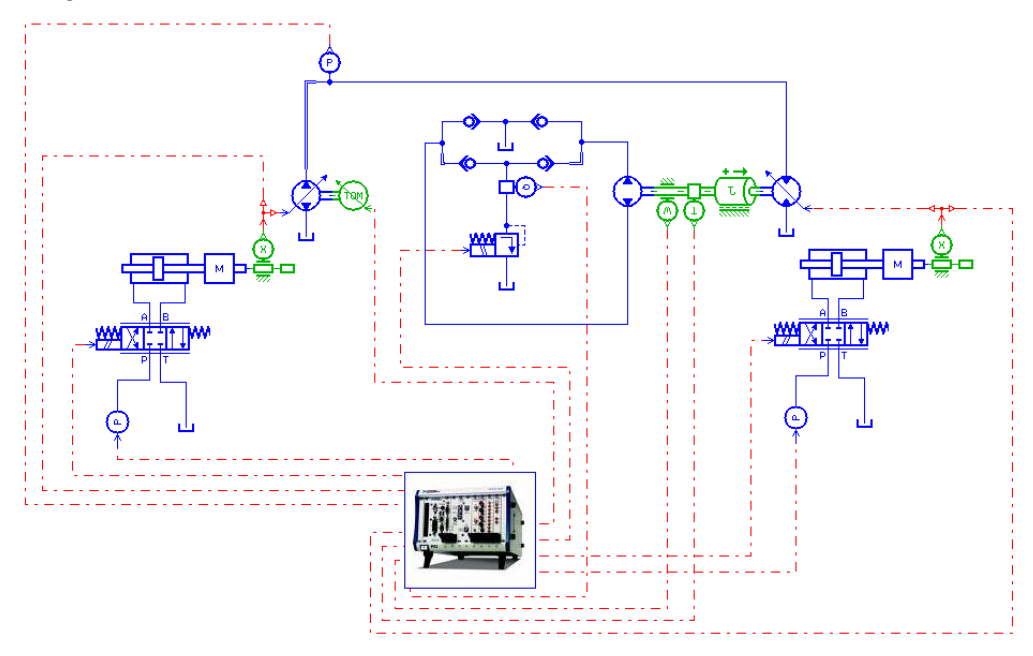


Fig.27- Mixed control hydrostatic transmission simulation network - detailed model.

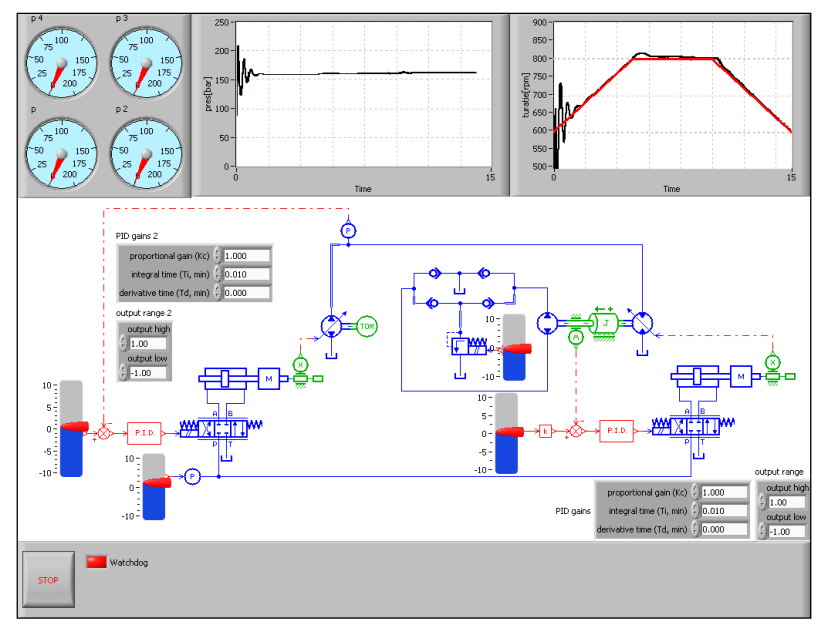


Fig.28- Virtual interface of the control model (LabVIEW / PXI).

The process computer used (PXI) runs the simulation network (real time model) with the automatic routines necessary to prescribe the numerical model references and acquire the data from the process. The acquired data is periodically sent to the process view system. Through the interface specific to the control process, which can be created on the PXI, an operator can order the change of the mathematical model input data.

The connection between the industrial computer and the experimental bench is made with the help of the dedicated interface boards of the PXI system. The connection is bidirectional; the computing system generates control signals and acquires the information necessary to close the internal calculation loops (feedback or feedforward). If one wants to run the mathematical model (simulator), simultaneously with the experimental bench control software model, the deterministic character of the mathematical model execution has to be taken into account.

3.5. Dynamic characteristics of mixed control hydrostatic transmission, achieved by numerical simulation

By running the AMESim simulation model of the hydrostatic transmission, the influence of some speed step signals, imposed on the adjustable hydraulic motor in the secondary side, on the control signals for adjusting the capacities of the two positive displacement machines, without and with error compensation, is highlighted.

A reference speed of 320 rpm has been established during the tests, which when exceeded, the transmission control system switches automatically from the pump capacity control to the hydraulic motor capacity control.

Increasing the hydraulic motor speed from zero to 320 rpm involves a control signal of the control system in order to increase the pump capacity. The variation of the hydraulic motor achieved speed, as an effect of this control signal, without and with error compensation, is shown in fig. 29.

Increasing the hydraulic motor speed from 320 rpm to 420 rpm involves a control signal of the control system in order to decrease the hydraulic motor capacity. The variation of the hydraulic motor achieved speed, as an effect of this control signal, without and with error compensation, is shown in fig. 30.

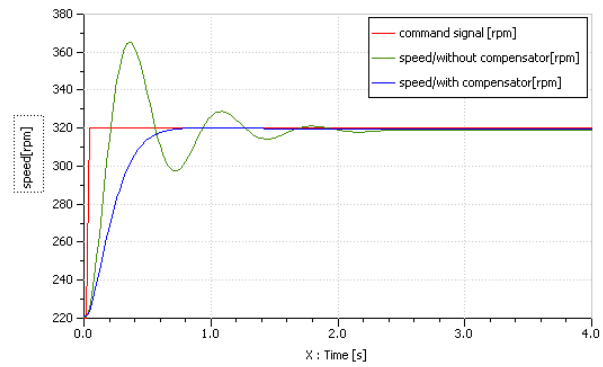


Fig.29- Response of hydraulic motor speed control system to excitation step signal –pump capacity control signal.

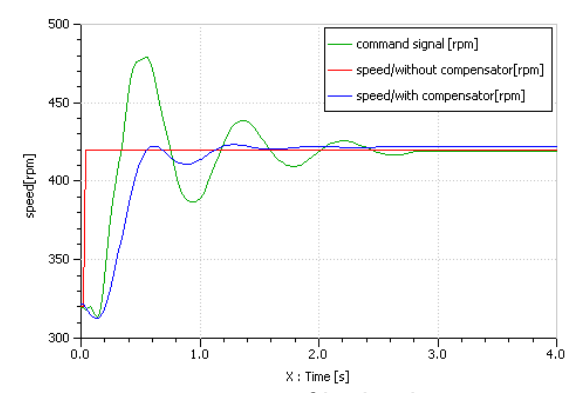


Fig. 30- Response of hydraulic motor speed control system to excitation step signal –motor capacity control signal.

3.6. Experimental validation of the hydrostatic transmission control model

For experimental validation of the hydrostatic transmission control model, the LabVIEW / PXI virtual control interface has been coupled to the physical transmission model. The hydraulic motor in the secondary side of the transmission has been excited with speed step and ramp signals.



The response of the transmission control system, which acts on the servomechanism of controlling the capacity of the pump in the primary side or on the servomechanism of controlling the capacity of the motor in the secondary side, depending on a predefined speed threshold (320 rpm), has been followed.

Dynamic characteristics of the system have been raised, which highlight:

- the influence of a speed step signal of 312 rpm, imposed on the adjustable hydraulic motor in the secondary side, on the adjustable pump capacity control, without and with error compensation, according to fig. 31;

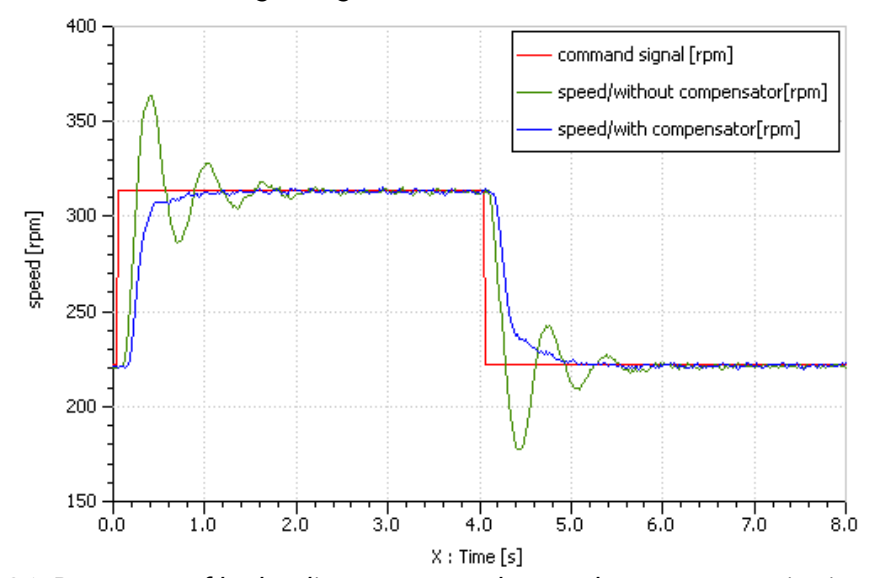


Fig.31- Response of hydraulic motor speed control system to excitation step signal pump capacity control signal.

- the influence of a speed step signal of 410 rpm, imposed on the adjustable hydraulic motor in the secondary side, on the adjustable motor capacity control, without and with error compensation, according to fig. 32;

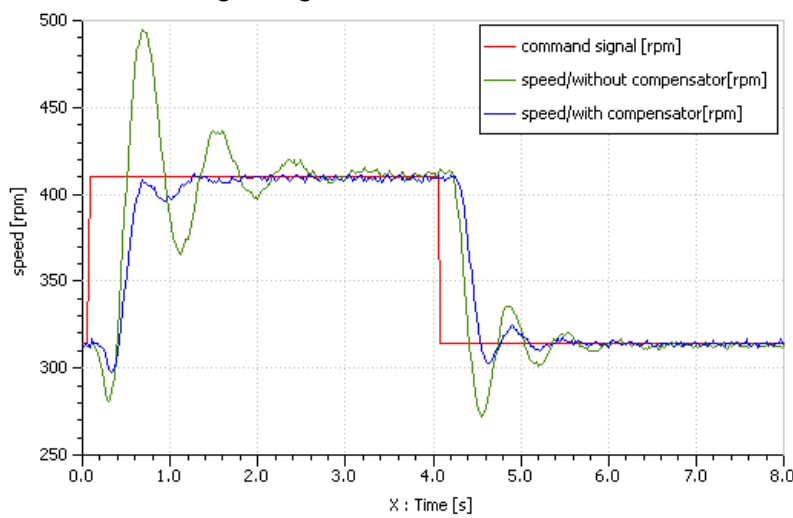


Fig.32- Response of hydraulic motor speed control system to excitation step signal – motor capacity control signal.

- the influence of combined speed step signals, of 308 rpm and 408 rpm, respectively, imposed on the adjustable hydraulic motor in the secondary side, on the adjustable



pump capacity control and the adjustable motor capacity control, respectively, without and with error compensation, according to fig. 33;

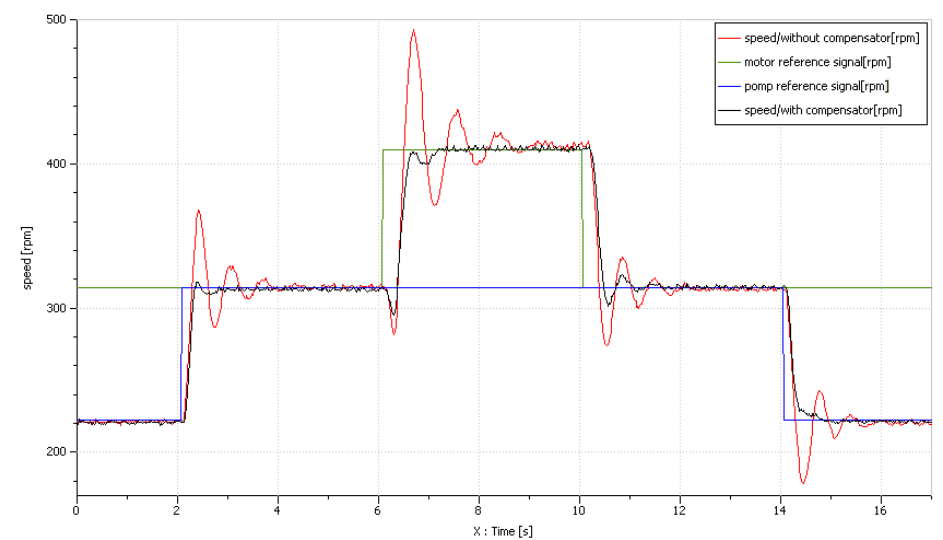


Fig.33- Response of hydraulic motor speed control system to combined excitation step signal – pump and motor capacities control signal.

- the influence of combined speed ramp signals, with maximum values of 315 rpm and 400 rpm, respectively, imposed on the adjustable hydraulic motor in the secondary side, on the adjustable pump capacity control and the adjustable motor capacity control, respectively, with error compensation, according to fig. 34.

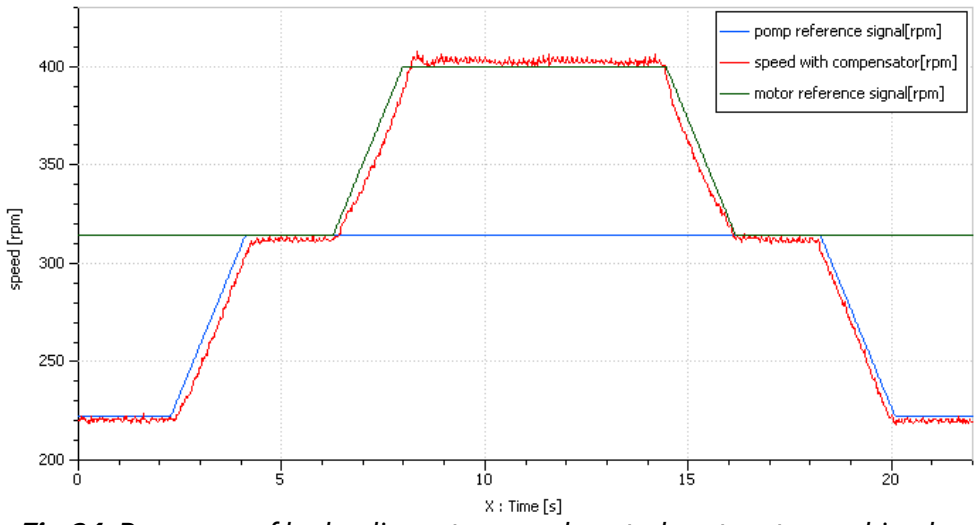


Fig.34- Response of hydraulic motor speed control system to combined excitation ramp signal – pump and motor capacities control signal.

The software application also includes a module for porting the experimental results data collected from the bench, via the Internet, using a web page. The online application also enables the control of process parameters – positive displacement pump capacity, hydraulic motor capacity and pressure rate in the load circuit. The web interface of the control model (LabVIEW / PXI), fig. 35, enables remote control of the hydrostatic transmission, namely laboratory testing of the transmission by persons outside the test laboratory.

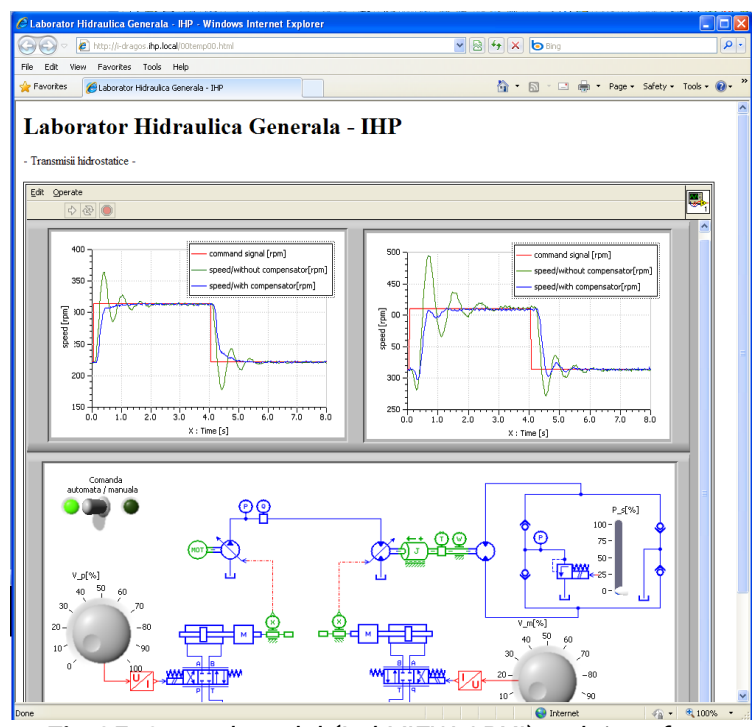


Fig.35- Control model (LabVIEW / PXI) web interface.

3.7. Conclusions on modeling, simulation and testing of mixed control hydraulic transmission

The control model of the mixed control hydraulic transmission has been tuned by successive iterations of simulations, performed in AMESim, and data processing, performed in LabVIEW.

The validation of the control model is confirmed by the shape of the experimentally raised characteristic curves, by coupling the LabVIEW / PXI virtual interface to the physical laboratory model, equivalent to the AMESim simulation model. Comparable dynamics, theoretically and experimentally identified, of the hydraulic transmission control system can be noted.

Obtaining control models for other hydraulic transmission configurations, with primary, secondary or mixed control, can be treated as a customization of this model achieved.

The possibility to use both mathematical models and real equipment enables tests to be conducted in research laboratories that would otherwise require *on-site* presence.

Cosimulation enales the simultaneous use of several modeling languages within the same simulation network. The use of this method of analysis is particularly useful in the development and design phases of complex automated systems, providing a quick solution to identify the characteristics of the analyzed system.

The current state of research in the field of hydrostatic transmissions reveals the need to use advanced simulation models for their systemic analysis.

By using advanced modeling and experimental identification procedures, superior dynamic performance for hydrostatic transmissions can be achieved.



4. Energy and functional advantages of adjustable hydraulic transmissions

4.1. Considerations regarding the energy advantages of adjustable hydraulic transmissions

In general, hydraulic transmissions based on positive displacement units, pumps and motors, of fixed capacity and on the laminar discharge of the excess flow through hydraulic resistances have good dynamic characteristics, but are disadvantageous from an energy point of view. Compared to these, hydraulic transmissions based on adjustable positive displacement units are energy efficient, but have less efficient dynamic characteristics.

In this sense, the chapter presents some aspects related to the energy advantages of the flow control based on hydraulic servo pumps, compared to the flow control based on fixed capacity hydraulic units, variable hydraulic resistances and laminar discharge of excess flow through pressure valves.

The chapter deals comparatively, from a theoretical and experimental point of view, with a hydraulic transmission with primary control, in which the flow in the primary side is controlled in two variants:

- the variant shown in fig. 36(a), in which a fixed capacity pump is used, the flow control is done with an adjustable throttle valve (losses across control valve), and the excess flow is discharged to the tank through a normally closed pressure valve (losses across relief valve);
- the variant shown in fig. 36 (b), in which an adjustable capacity hydraulic servo pump is used.

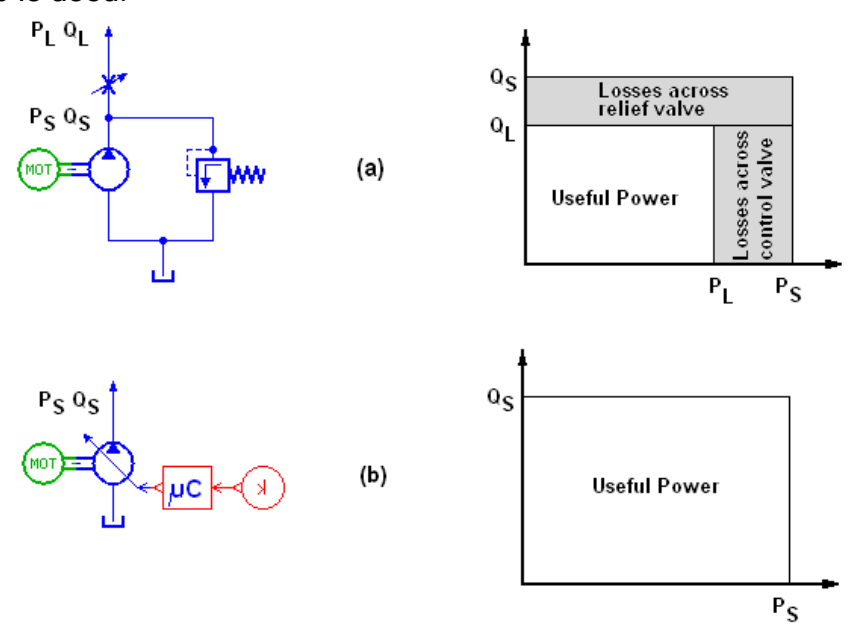


Fig.36- Flow control in hydraulic transmissions: (a)- with fixed capacity pump; (b) with hydraulic servo pump.

The useful power in the variant shown in fig. 36(a) is lower than the useful power in the variant shown in fig. 36(b), due to the loss of pressure across the throttle valve and the discharge of excess flow through the relief valve.



4.2. Basic model and numerical simulation network of primary control hydraulic transmission

Transmission analysis has been performed using two distinct modeling / simulation and process control environments: AMESim and LabVIEW. The cosimulation model comprises a numerical simulation network of the hydrostatic unit, which operates in pump mode (RKP-D type Moog / radial piston pump) and an open circuit hydrostatic transmission simulation network consisting of two hydrostatic units with adjustable capacity.

The analyzed primary control hydrostatic transmission, with a single consumer of the rotary, adjustable positive displacement motor type, according to fig. 37, comprises:

in the primary side: MOOG servo pump, item 1, with radial pistons and integrated electronics, with three control loops, namely (1) in flow, (2) in pressure, and (3) in flow and pressure; electric motor for driving the servo pump, constant speed, item 2; pressure limiting valve, item 3; flow transducer, item 4; pressure transducer, item 5; adjustable throttle valve, item 15.

in the secondary side: BOSCH servomotor, item 7, with axial pistons, bent-axis and integrated electronics, used as a fixed capacity unit; torque transducer, item 8; speed transducer, item 9; axial piston pump, bent-axis, fixed capacity, item 10, to simulate the load of the hydraulic servomotor; two pressure transducers, item 11 and item 13; four check valves, item 12, mounted on the suction / discharge of the load pump; pressure control valve with proportional electrical control, item 14, to control the load of the hydraulic servomotor.

a PXI-NATIONAL INSTRUMENTS **block**, item 6, which provides the virtual interface for the process of controlling the capacity of adjustable positive displacement machines (LabVIEW / PXI).

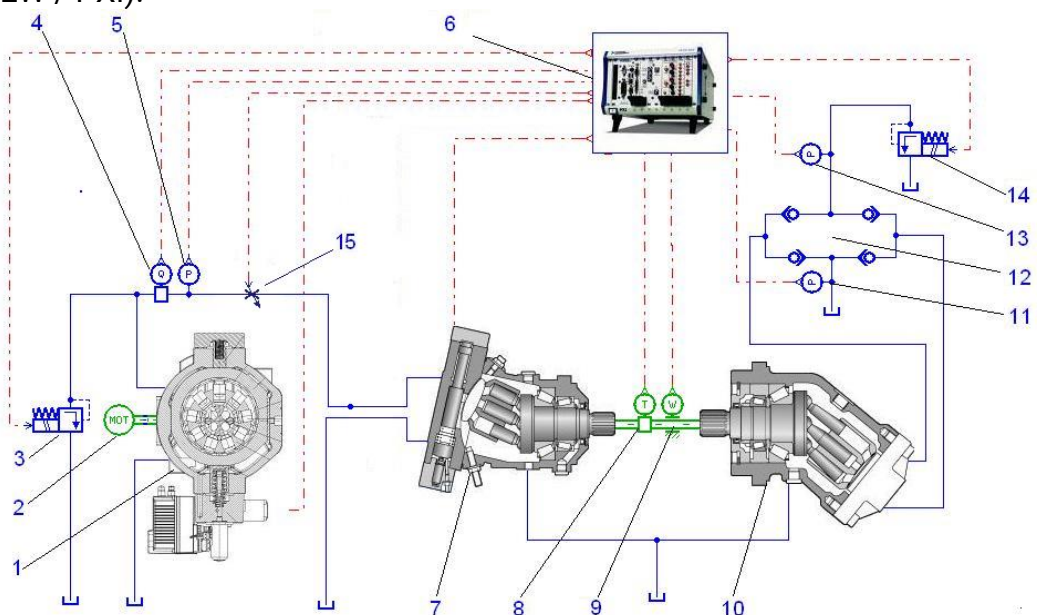


Fig. 37- Hydrostatic transmission simulation network - basic model.

The radial piston positive displacement pump model has been integrated into the hydrostatic transmission simulation network. The transmission comprises the hydrostatic unit operating in pump mode, the positive displacement motor with adjustable capacity and the module consisting of fixed capacity hydrostatic pump, pressure relief valve and directional valve block; this module is used as a hydrostatic load. The hydraulic system is controlled by the NI-PXI process computer; with its help various schemes for controlling the transmission parameters can be implemented.

The application implemented on the numerical computing system is an AMESim / LabVIEW cosimulation model, the model developed in AMESim simulating the operation of the hydraulic and mechanical components of the process, and the software component - the numerical control part.

The cosimulation process enables the coupling of the control software component to the simulated process model, for preliminary tuning of the controller parameters; they continue to serve as reference parameters for the fine-tuning stage performed on the experimental bench.

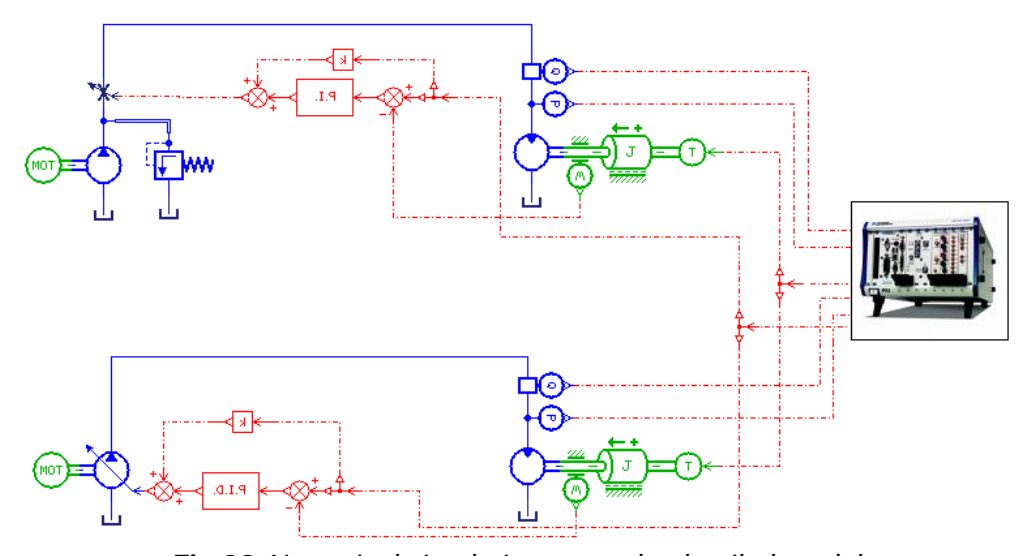


Fig.38- Numerical simulation network - detailed model.

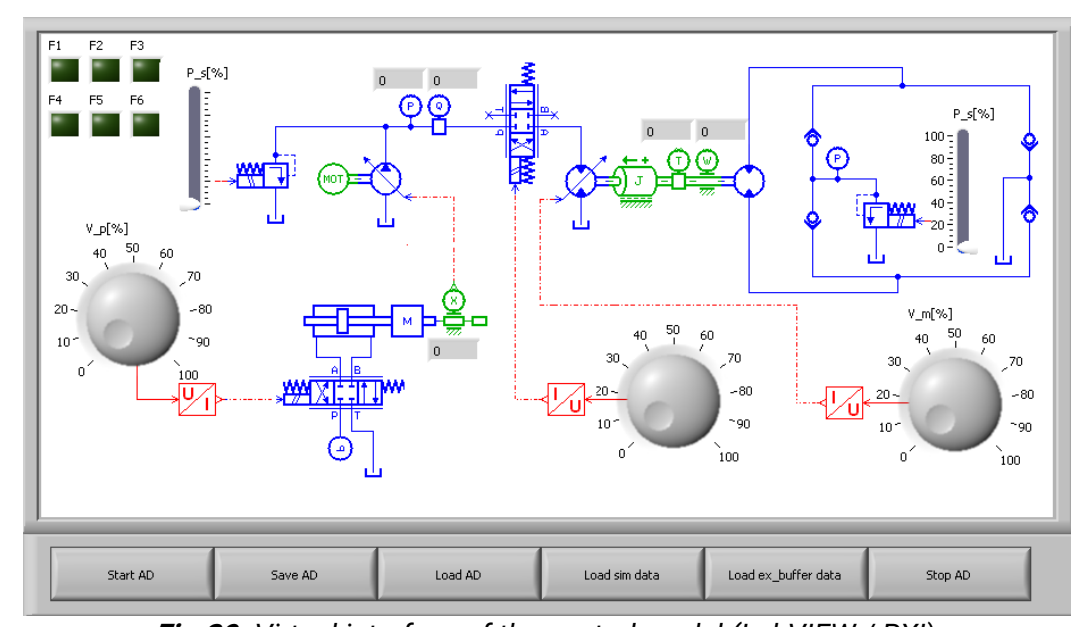


Fig.39- Virtual interface of the control model (LabVIEW / PXI).

Fig. 38 shows the detailed model of the numerical simulation network for the primary control hydrostatic transmission, made with the help of the AMESim software program, and fig. 39 - the virtual interface of the transmission control model, made with the help of the LabVIEW software program and a PXI-NATIONAL INSTRUMENTS module.

4.3. Energy efficiency analysis of hydraulic transmissions with fixed or adjustable capacity pumps

After calibration of the transmission control model with primary control, performed using the numerical simulation network, the motor in the secondary side has been set to maximum capacity, and the two flow control systems for the pump in the primary side have been compared. The tests have been performed for a constant load of 20Nm on the hydraulic motor shaft in the secondary side of the transmission.

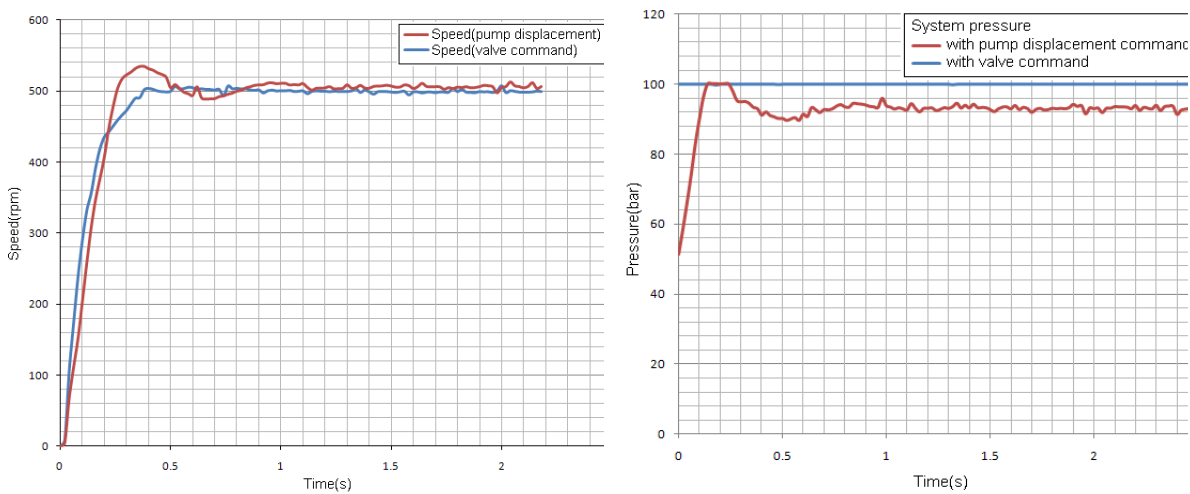


Fig.40(a)- Variation in the speed of hydraulic motor in the secondary side to excitation step signal of primary flow control systems.

Fig.40(b)- Variation in the pressure on the primary circuit to excitation step signal of primary flow control systems.

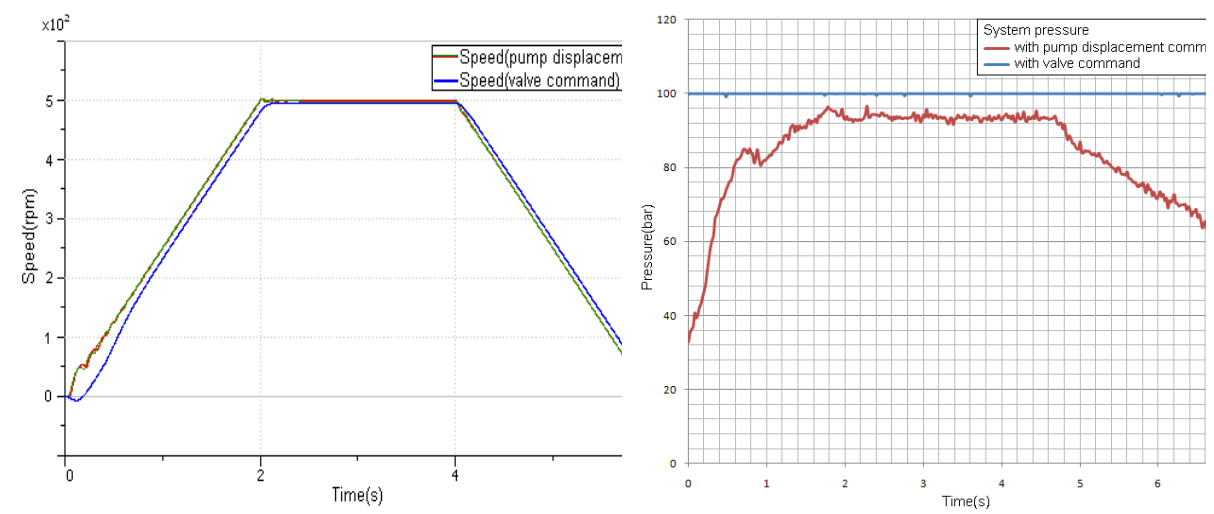


Fig.41(a)- Variation in the speed of hydraulic motor in the secondary side to excitation ramp signal of primary flow control systems.

Fig.41(b) Variation in the pressure on the primary circuit to excitation ramp signal of primary flow control systems.



Experimentally, the two systems were cyclically excited, with and without energy efficiency, with speed step type (500 rpm), fig. 40, and ramp type control signals, fig. 41. The evolution of the hydraulic motor shaft speed, fig. 40(a), fig.41(a), and pressures in the primary hydraulic circuit, fig. 40(b), fig. 41(b) have been recorded over time.

The two systems controlling the flow in the primary side of the transmission have been excited with a signal controlling the speed of hydraulic motor in the secondary side, corresponding to a specific, predefined profile. Circuit pressures have been recorded, fig. 42 (in blue- hydraulic motor speed variation; in brown- variation of hydraulic motor supply pressure in an energy efficient system; in red- variation of hydraulic motor supply pressure in an energy inefficient system).

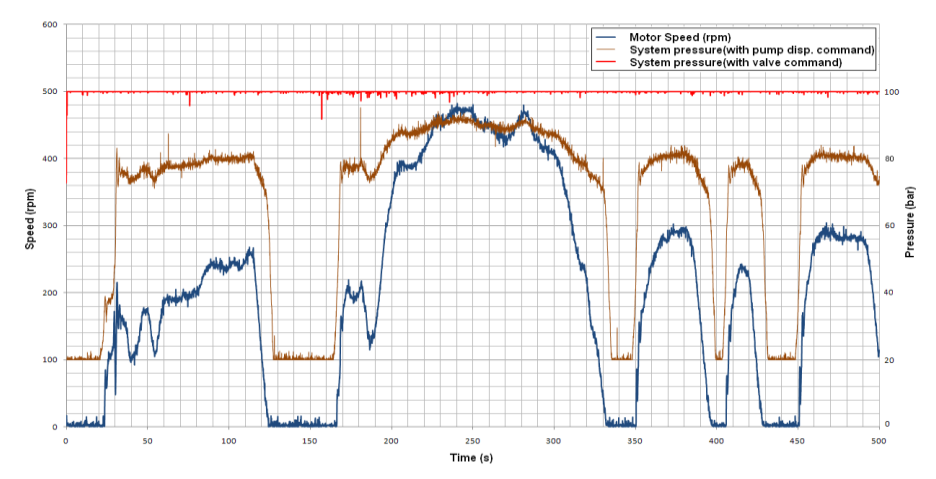


Fig.42- Pressure variation on the primary circuit of the hydraulic transmission at a control signal with a predefined profile for the speed of the motor in the secondary side.

In fig.43, after calculating the hydraulic power consumed by the pump in the primary side (P=Q*p), the time evolutions of this power for the two flow control systems have been depicted, without (in brown) and with (in blue) energy efficiency. The obtained data have been numerically integrated to obtain the evolution of the consumed energy, fig. 44 (in brown- energy inefficient system; in blue- energy efficient system).

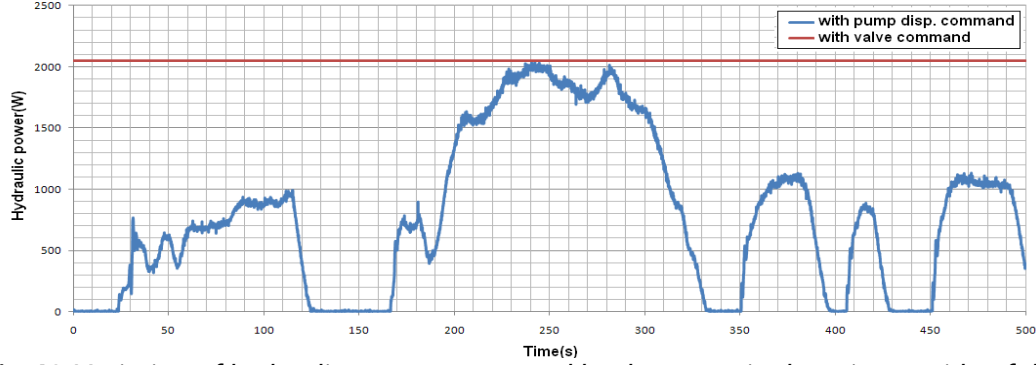


Fig.43- Variation of hydraulic power consumed by the pump in the primary side of the transmission, at a control signal with a predefined profile for the speed of the motor in the secondary side.



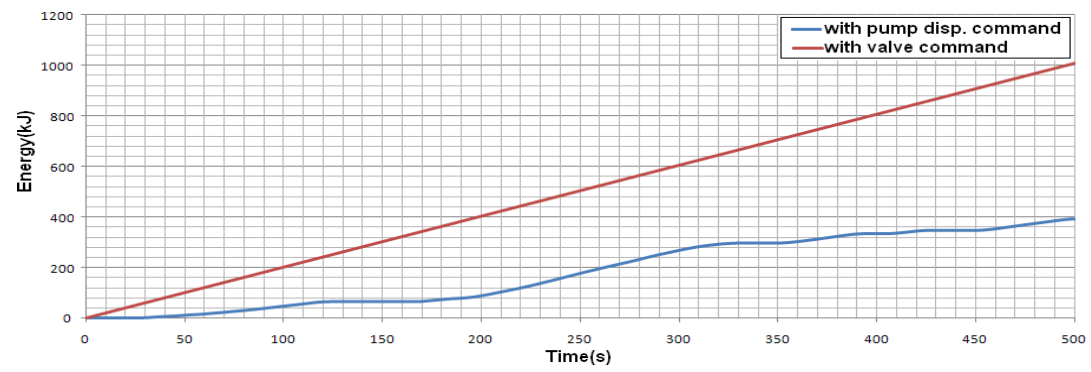


Fig.44 Variation of energy consumed by the pump in the primary side of the transmission, at a control signal with a predefined profile for the speed of the motor in the secondary side.

4.4. Conclusions on the energy efficiency of hydraulic transmissions with fixed or adjustable capacity pumps

In the case of the analyzed hydraulic transmission, for which the hydraulic motor in the secondary side of the transmission, with constant shaft resistance torque (20Nm), is controlled with a signal with a random, predefined profile, the following conclusions can be drawn:

- the energy consumed by the pump in the primary side of the hydrostatic transmission, when using a Moog RKP-D hydraulic servo pump, is obviously smaller than when using a fixed capacity pump, with flow control by variable hydraulic resistance and discharge of excess flow across the valve;
- the energy saved is given by the area of the surface delimited by the two curves (brown and red) in fig. 44 above;
- the flow control system, based on the use of this servo pump, has a small time constant in transient mode (approx. 0.2s in the case under analysis), which depends on the hydraulic motor load.

From the point of view of energy consumption and dynamic performance, the application can be extended to the analysis of secondary control of the transmission (performed on the hydraulic servomotor) and to the analysis of mixed control (performed on the servo pump in the primary side and on the hydraulic servomotor in the secondary side).



5. Virtual tests on secondary control hydraulic transmissions

5.1. Secondary control hydraulic transmission with fixed capacity pump and variable capacity motor

5.1.1. Mathematical modeling of hydraulic transmission

Mathematical modeling has been performed for a secondary control hydraulic drive system (obtained by customizing the system developed), which has in its structure the following main subassemblies:

- pressure source, made of a fixed capacity positive displacement pump, driven at constant speed;
 - execution element, made of an adjustable capacity hydraulic motor;
- load simulation module, made of a fixed capacity positive displacement pump and a proportional pressure control valve.

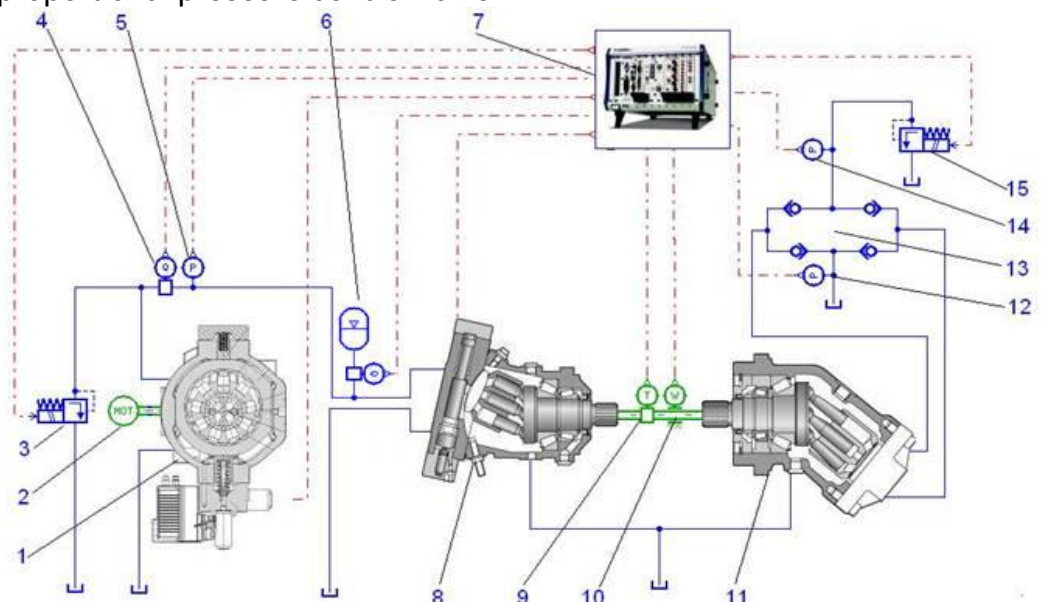


Fig.45 Schematic diagram of a mixed, primary or secondary control hydraulic transmission.

In order to perform the mathematical modeling, the characteristic equations of each equipment have been written, as well as the connection relations between the main pieces of equipment.

This system has been tested in the Fluid Power Laboratory of INOE 2000-IHP Bucharest. It is a mixed control hydraulic transmission, with adjustable positive displacement machines in the primary and secondary sides, with the possibility of using the primary control, by locking the capacity of the hydraulic motor in the secondary side to a constant value, or the secondary control, by locking the capacity of the pump in the primary side to a constant value. The schematic diagram of the system is shown in fig. 45.

5.1.1a. Flow rate discharged from the pump

Theoretical flow rate of a fixed capacity positive displacement pump is determined using the equation:

$$Q_{tp} = V_p \cdot N_p \tag{1}$$

where,

- Q_{tp} stands for theoretical pump flow rate, expressed in $[m^3/s]$;
- V_p stands for maximum pump capacity, expressed in [m³/rev];
- N_n stands for pump speed, expressed in [rev/s].

Pump *leakage flow rate* is determined, accepting the hypothesis of laminar fluid flow, using the equation:

$$Q_{sp} = K_{sp} \cdot P \tag{2}$$

where,

- Q_{sp} stands for pump leakage flow rate, expressed in [m^3/s];
- K_{sp} stands for pump leakage coefficient, expressed in $[m^5/N.s]$;
- P stands for pump discharge pressure, expressed in [N/m²].

Discharge flow rate from the pump is the difference between theoretical pump flow rate and pump leakage flow rate, and it is determined using the equations:

$$Q_p = Q_{tp} - Q_{sp} \tag{3}$$

and further,

$$Q_p = V_p \cdot N_p - K_{sp} \cdot P. \tag{4}$$

5.1.1b. Flow rate consumed by the motor

Theoretical flow rate of a rotary hydraulic motor is determined using the equation:

$$Q_{tm} = V_m \cdot N_m \cdot X \tag{5}$$

where,

- Q_{tm} stands for theoretical motor flow rate, expressed in $[m^3/s]$;
- V_m stands for motor capacity, expressed in [m^3/rev];
- $N_{\scriptscriptstyle m}$ stands for motor speed, expressed in [rev/s];
- X stands for a dimensionless parameter, with values in the range [0 ... 1].

Motor *leakage flow rate* is determined, accepting the hypothesis of laminar fluid flow, using the equation:

$$Q_{sm} = K_{sm} \cdot P \tag{6}$$

where,

- Q_{sm} stands for motor leakage flow rate, expressed in [m^3/s];
- K_{sm} stands for motor leakage coefficient, expressed in [$m^5/N.s$];
- P stands for motor supply pressure, expressed in $[N/m^2]$.

Flow rate consumed by a rotary hydraulic motor is the sum of theoretical flow rate and leakage flow rate, and it is determined using the equations:

$$Q_m = Q_{tm} + Q_{sm} \tag{7}$$

and further,

$$Q_m = V_m \cdot N_m \cdot X + K_{sm} \cdot P \tag{8}$$

If one ignores the pressure losses across the pipes and the connection fittings between the pump and the motor, then one can admit that the discharge pressure of the pump is equal to the supply pressure of the motor.

5.1.1c. Continuity equation

The continuity equation, specific to hydraulic transmissions, has the form:

$$Q_p - Q_m = \frac{V_0}{E} \cdot \frac{dP}{dt} \tag{9}$$

where.

- V_0 stands for total volume of pressurized oil (half the capacity of the hydraulic pump, half the capacity of the hydraulic motor, and the volume of oil in the connecting pipes between the pump and the motor), expressed in $[m^3]$;
 - E_e stands for equivalent bulk modulus, expressed in [Pa].

5.1.1d. Torque developed by the hydraulic motor

The torque developed by the hydraulic motor is calculated using the equation:

$$M_{m} = \frac{V_{m} \cdot P}{2 \cdot \pi} \tag{10}$$

where,

- M_{m} - stands for torque developed by the motor, expressed in [N.m].

5.1.1e. Equilibrium of moments equation

The torque developed by the hydraulic motor must be equal to the sum of the torque due to inertia, the torque developed by the friction forces and the resistance torque.

$$\frac{V_m \cdot P(s)}{2 \cdot \pi} = J \cdot \frac{d^2 \theta}{dt^2} + K_f \cdot \frac{d\theta}{dt} + M_r \tag{11}$$

where,

- J stands for total moment of inertia, reduced to the motor shaft, of moving parts, expressed in $[kg.m^2]$;
 - K_f viscous friction coefficient, expressed in [N.m.s];
 - θ angle traveled by the motor shaft, expressed in [degrees];
 - M_{Γ} resistance torque, expressed in [N.m].

If we denote angular speed of the hydraulic motor shaft by " ω ", then between parameters θ and ω there are the following relations:

$$\omega = \frac{d\theta}{dt} \tag{12}$$

$$\dot{\omega} = \frac{d^2\theta}{dt^2} \tag{13}$$

$$\omega = 2 \cdot \pi \cdot N_{m} \tag{14}$$

Under these conditions, eqation (11) becomes:

$$\frac{V_m}{2 \cdot \pi} \cdot P(s) = J \cdot \dot{\omega} + + K_f \cdot \omega + M_r \tag{15}$$

$$\frac{V_m}{2 \cdot \pi} \cdot P(s) = J \cdot 2 \cdot \pi \cdot \dot{N}_m + K_f \cdot 2 \cdot \pi \cdot N_m + M_r \tag{16}$$

The resistance torque is variable over time and can have any shape, linear or nonlinear.

5.1.1f. Characteristic of the pressure relief valve

The value of the system pressure, adjusted by means of the pressure relief valve, is described by the equation:

$$p = k_{s} \cdot U \tag{17}$$

where,

- p stands for controlled pressure value, expressed in [Pa];
- k_s stands for the constant of the valve, expressed in [Pa/V];
- U- stands for valve control voltage, expressed in [V].

5.1.1g. Characteristic of the speed transducer

The characteristic of the speed transducer is given by the equation:

$$U = k_t N \tag{18}$$

where,

- N stands for speed value, expressed in [rot/min];
- k_t- stands for the constant of the transducer, expressed in [V/rev/min];
- U stands for transducer output voltage, expressed in [V].

5.1.1h. Characteristic of the torque transducer

The characteristic of the torque transducer is given by the equation:

$$U = k_{m}M \tag{19}$$

where,

- M stands for torque value, expressed in [Nm];
- k_m- stands for the constant of the transducer, expressed in [V/Nm];
- U stands for transducer output voltage, expressed in [V].

5.1.1i. Characteristic of the hydroaccumulator

The characteristic of the hydroaccumulator has been considered for adiabatic transformation:

$$pV^k = ct. (20)$$

where,

- p stands for air pressure value, expressed in [Pa];
- V- stands for volume of gas in the hydroaccumulator, expressed in [m³];
- k stands for the adiabatic coefficient.

5.1.2. Numerical simulation of hydraulic transmission

The numerical simulation of the operation of a secondary control hydraulic drive system (transmission) has been performed using the AMESim simulation software package. The numerical values of the parameters of the pieces of equipment in the structure of the system are presented in Table 1. The simulations have been performed on the assumption that the main pump (in the primary side) has a fixed capacity, to highlight the variation of hydraulic motor (in the secondary side) capacity.

Item no.	Parameter name	Value	Notes
1	Maximum capacity of main pump V_p [cm ³ /rev]	32	
2	Pump speed N _p [rev/min]	1450	
3	Rated value of pump discharge pressure P_{pnom} [bar]	315	
4	Pump leakage flow rate at rated pressure value $Q_{scp}[I/min]$	0.5	
5	Motor capacity V _m [cm ³ /rev]	28	variable
6	Motor speed N _m [rev/min]	-	variable
7	Rated value of motor supply pressure $P_{mnom}[bar]$	315	variable
8	Motor leakage flow rate at rated pressure value $Q_{scm}[l/min]$	1	
9	Moment of inertia of motor driven parts $J[Kg.m^2]$	0.05	
10	Volume of pressurized oil V ₀ [l]	5	
11	Equivalent bulk modulus <i>E_e[bar]</i>	14.000	
12	Hydroaccumulator volume V _h [l]	2.5	
13	Rated value of valve control voltage <i>U [V]</i>	10	variable
14	Load pump capacity V_p [cm ³ /rev]	14	

Tab. 1- Values of the main parameters in the system structure.

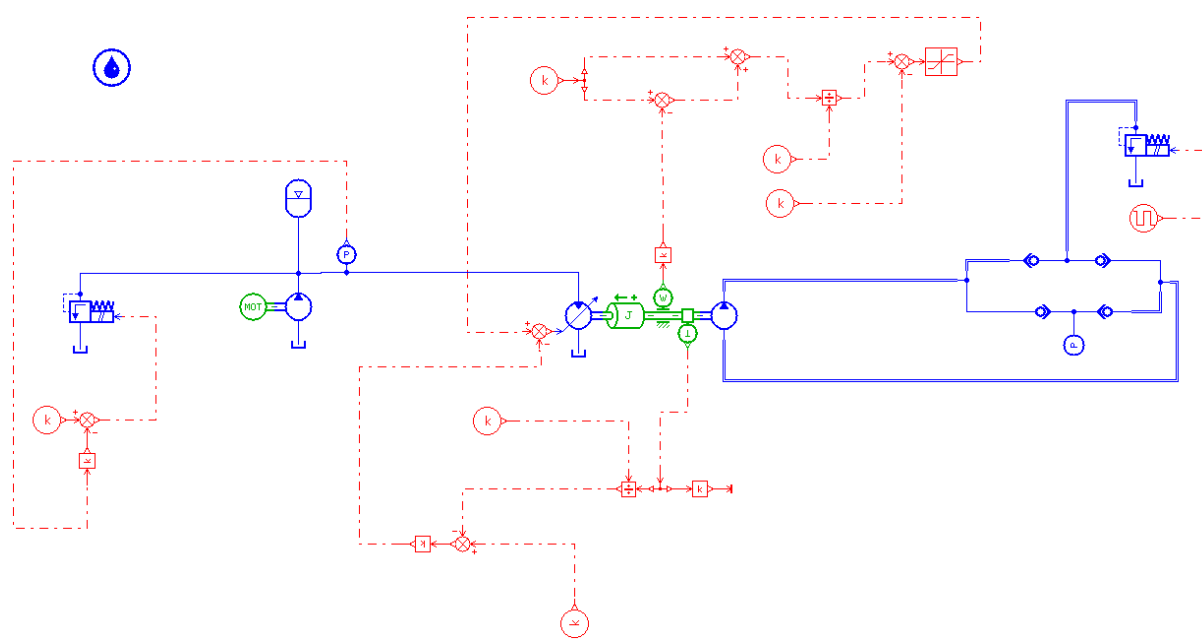


Fig.46- Simulation model of secondary control hydraulic drive system.

The network of the system simulation model, developed in AMESim, is shown in fig. 46, and the results of numerical simulations are shown in figures 47...58.

The simulation model (fig. 46), developed in AMESim, contains a control loop for the capacity of hydraulic motor in the secondary of the transmission (system),



depending on the resistance torque at its shaft, under the conditions of supplying this motor at constant pressure and in order to reduce the speed variation depending on the variation of the motor load.

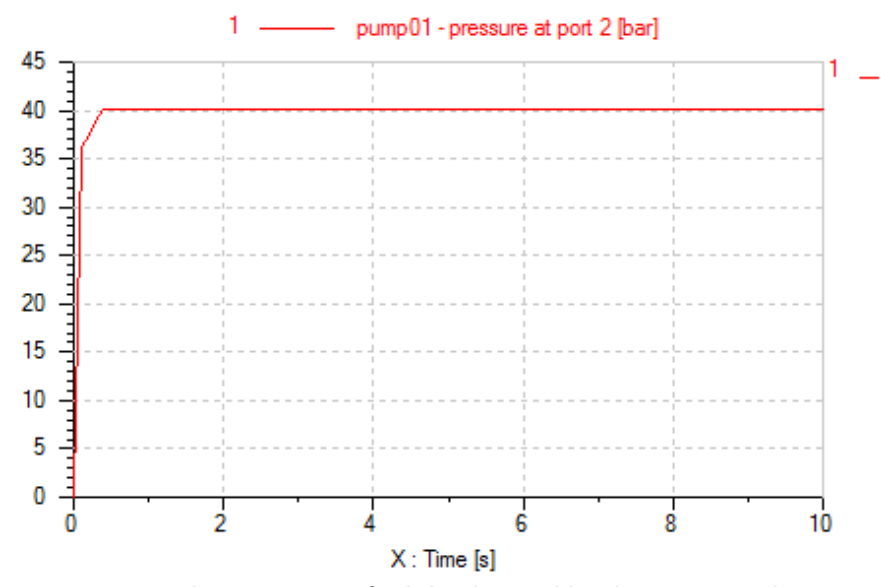


Fig.47- Variation in the pressure of oil discharged by the pump in the primary.

In fig. 47 one can notice that the pressure discharged by the pump in the primary of the transmission is approximately constant (secondary control) throughout the excitation time of the proportional valve, corresponding to the load simulation pump, with a rectangular signal. The stabilization time at 40 bar of the discharge pressure of this pump is approximately 0.4 s.

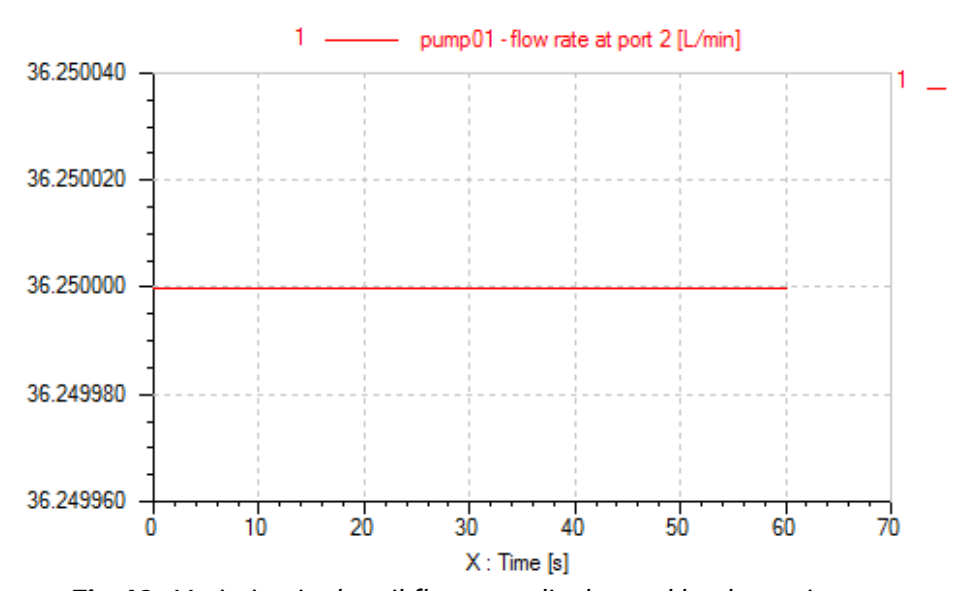


Fig.48- Variation in the oil flow rate discharged by the main pump.

In fig. 48 one can notice that, throughout the simulation, the pump in the primary side discharges a constant flow rate of 36.25 l / min.

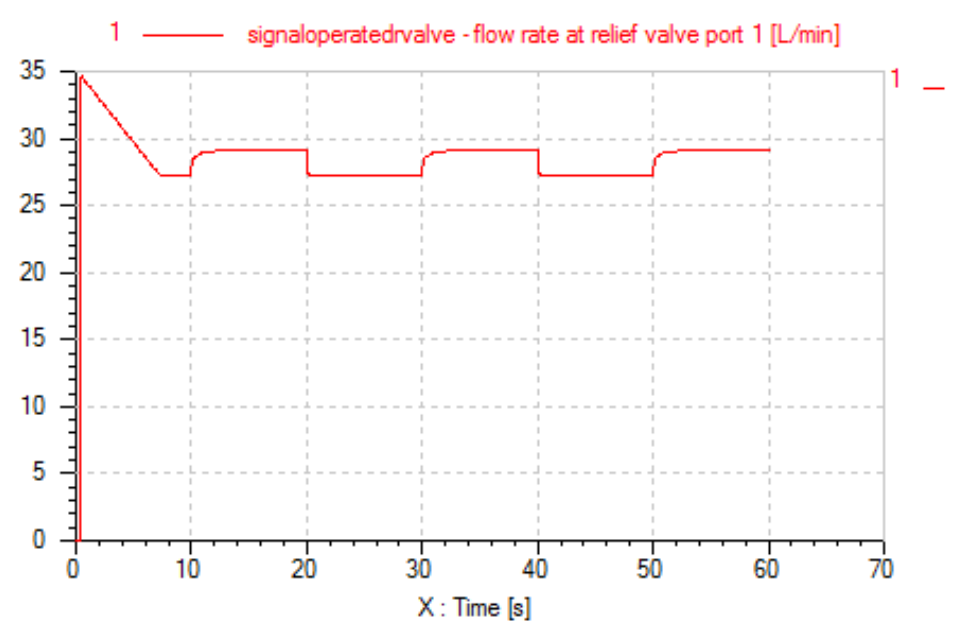


Fig. 49- Oil flow rate variation across pressure relief valve.

A flow rate varying in the range of 35 ... 27 l / min is discharged through the pressure relief valve, corresponding to the pump in the primary, over the simulation interval of 0 ... 6 s, and in the range of 27 ... 29 l/min, over the rest of the time interval, see fig. 49. Depending on the variation in the load of the hydraulic motor in the secondary side, the flow rate variation interval is interrupted by constant flow rate intervals.

The relatively high value of the flow rate discharged through the valve is one of the reasons why this control model has to be optimized, in terms of energy.

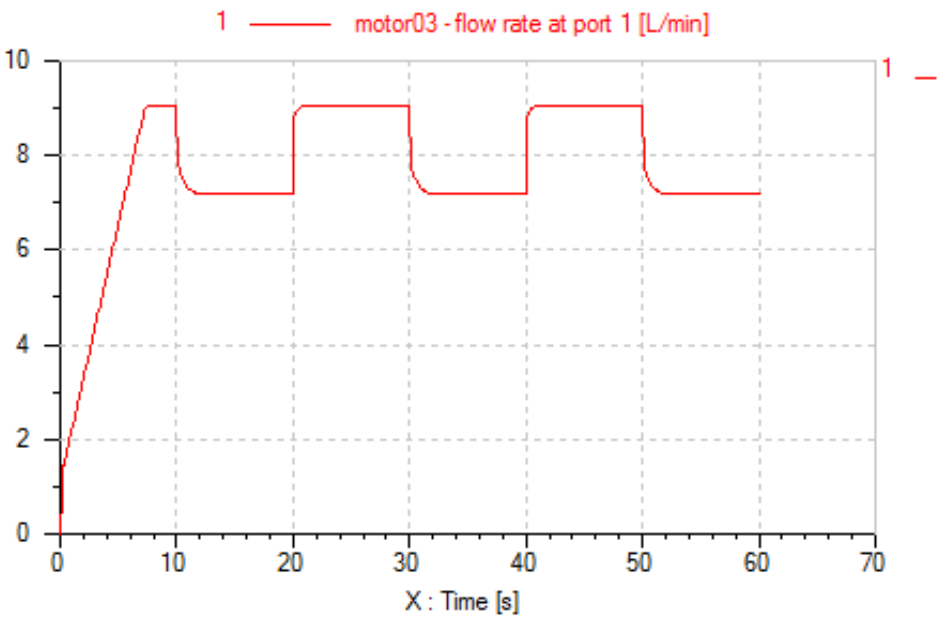


Fig. 50- Oil flow rate variation at hydraulic motor supply connection.

Variation in oil flow rate at the supply connection of the hydraulic motor in the secondary side, acc. to fig. 50, is of 0...9 l/min, over the interval of 0...6 s, and of 9...7.2



I/min, over the rest of the time interval. Depending on the variation in the load of the hydraulic motor in the secondary side, the flow rate variation interval is interrupted by constant flow rate intervals.

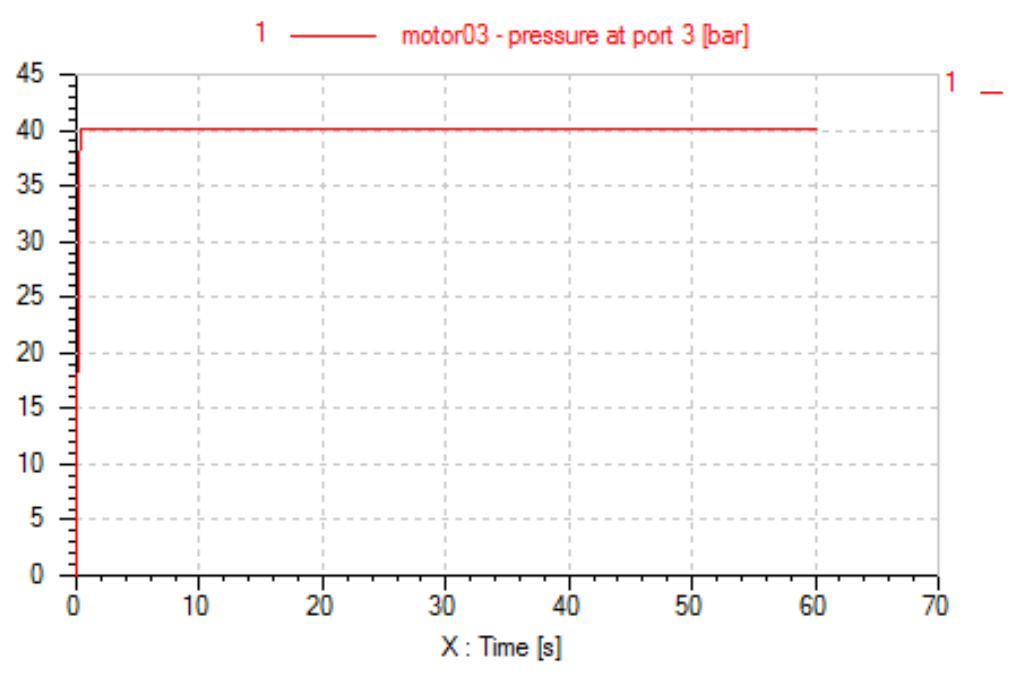


Fig.51- Oil pressure variation at motor supply connection.

Throughout the simulation, oil pressure at hydraulic motor supply connection has a value of 40 bar, acc. to fig. 51. Supply of the hydraulic motor at constant pressure is a condition of the secondary control.

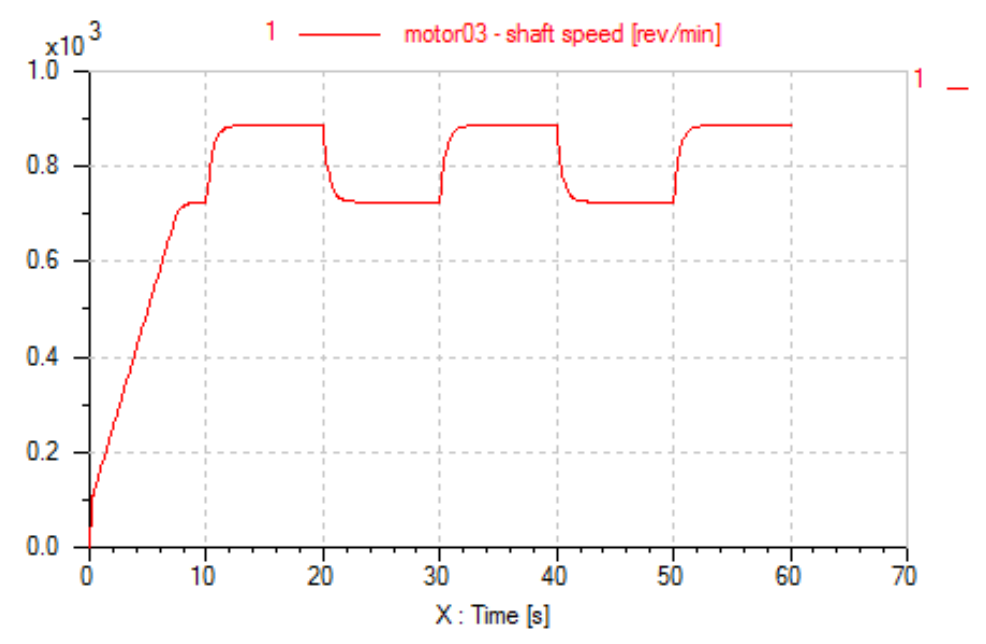


Fig.52- Hydraulic motor speed variation.

The speed of the hydraulic motor in the secondary side varies in the range of 0 ... 720 rpm, over the interval of 0...7 s, and in the range of 720...900 rpm, over the rest

of the time interval, acc. to fig. 52. Depending on the variation in the load of the hydraulic motor in the secondary side, the speed variation interval is interrupted by constant speed intervals.

The relatively large variation in motor speed is another reason why this control model needs to be optimized, in terms of functionality.

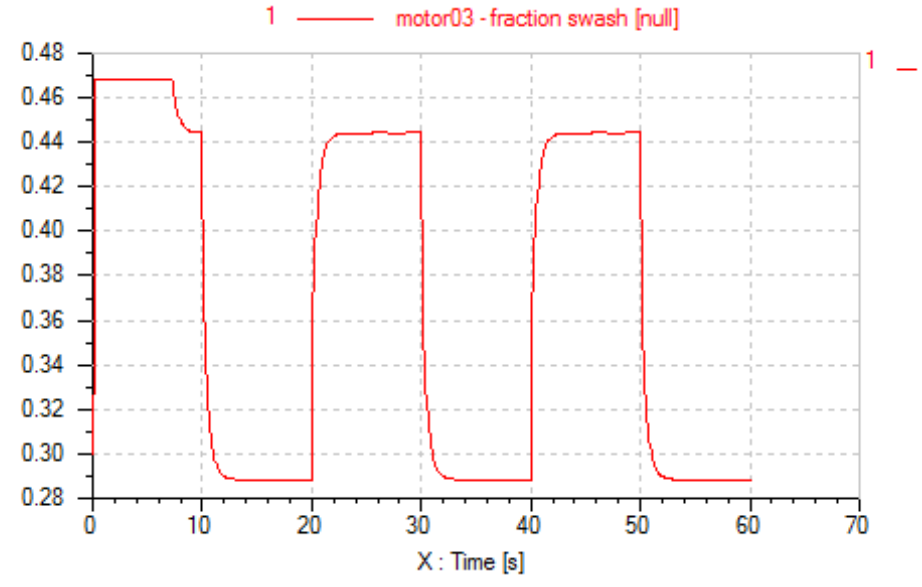


Fig.53- Hydraulic motor capacity variation.

The capacity of the hydraulic motor in the secondary side of the transmission varies in the range of 0 ... 0.47 of the maximum capacity, over the interval of 0...7 s, and in the range of 0.47...0.28 of the maximum capacity, over the rest of the time interval, acc. to fig. 53. Depending on the variation in the load of the hydraulic motor in the secondary side, the capacity variation interval is interrupted by constant capacity intervals.

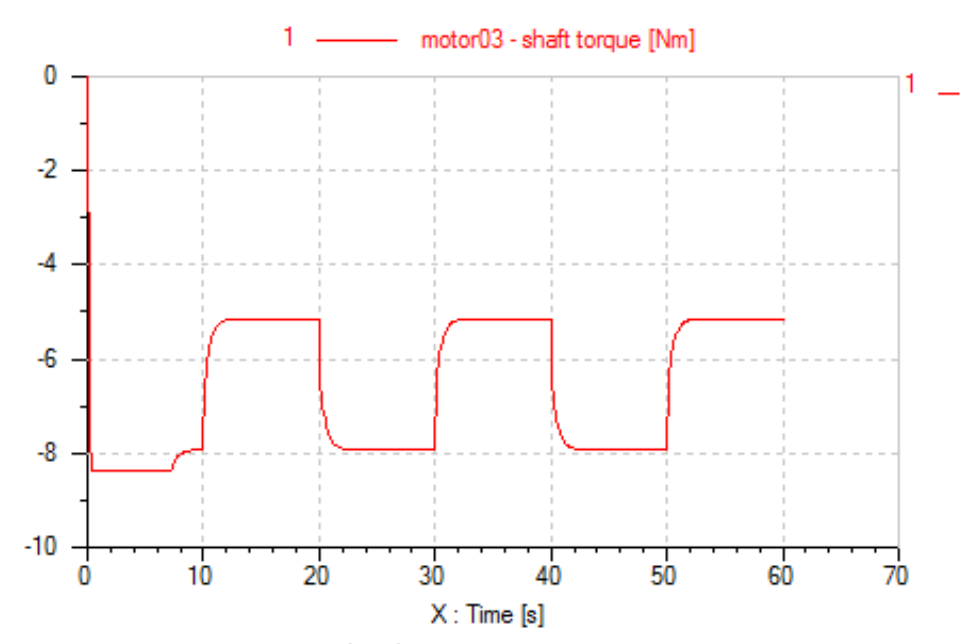


Fig. 54- Hydraulic motor torque variation.



The resistance torque at the shaft of the hydraulic motor in the secondary side varies in the range of 0 ... 8.4 Nm, over the interval of 0...7 s, in the range of 8.4...8 Nm, over the interval of 7...10 s and in the range of 8...5 Nm, over the rest of the time interval, acc. to fig. 54. Depending on the variation in the load of the hydraulic motor in the secondary side, the torque variation interval is interrupted by constant torque intervals.

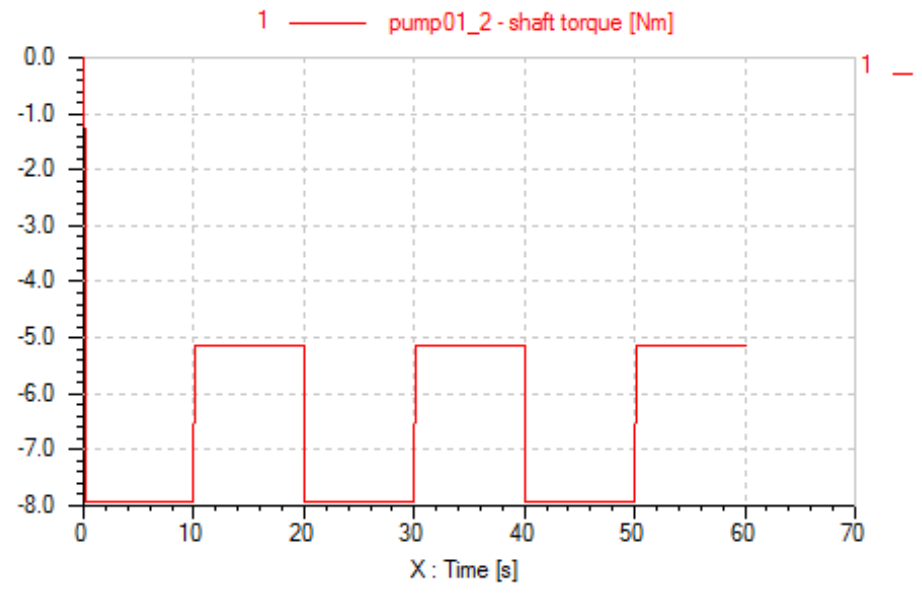


Fig. 55- Variation in the resistance torque generated by the load pump.

During the simulation, the load pump generates a step resistance torque, with max. Val.= 8 Nm, min. Val.= 5 Nm and Duration_{max.Val./mim.Val.} =10 s, acc. to fig. 55.

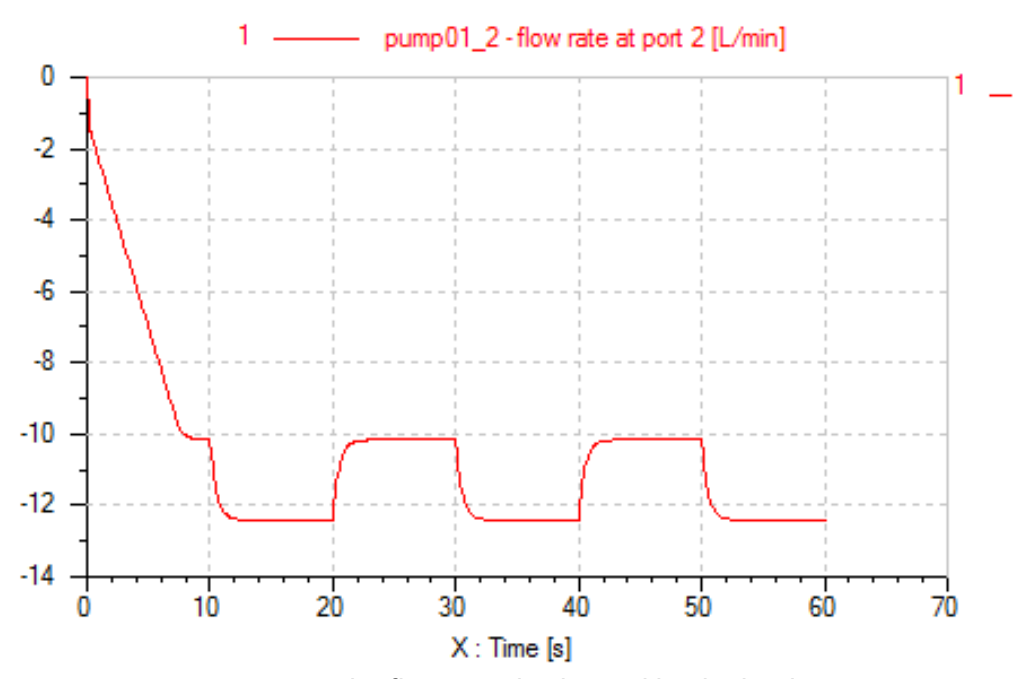


Fig.56- Variation in the flow rate discharged by the load pump.

During the generation of the resistance torque, the flow rate discharged by the load pump varies acc. to fig.56.



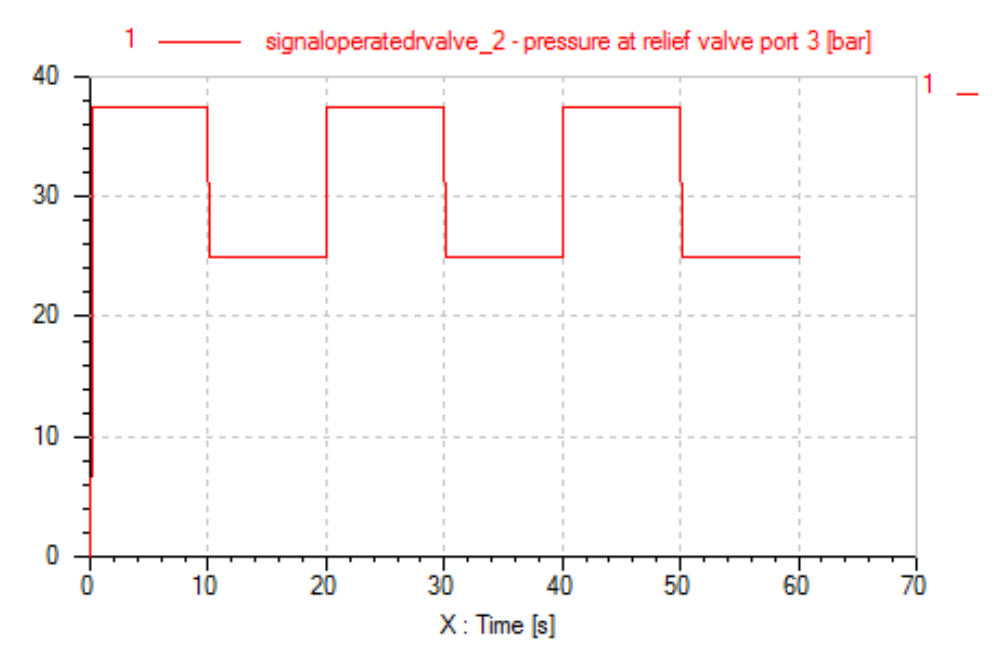


Fig.57- Oil pressure variation at the pressure connection of the load pressure relief valve.

In order for the load pump to generate the resistance torque, acc. to fig. 56, in the pressure relief valve, corresponding to the load pump, the pressure has to vary acc. to fig. 57. This condition has been met by exciting the proportional pressure relief valve, during the simulation, with a rectangular signal.

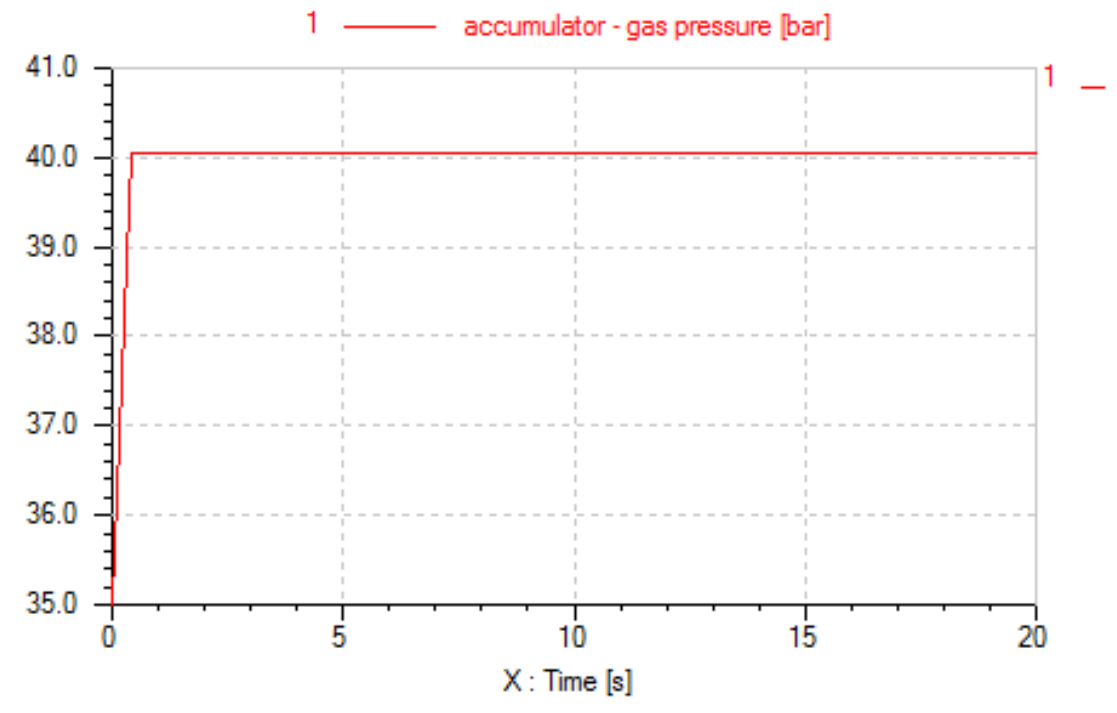


Fig. 58- Variation of gas pressure in the hydroaccumulator.

After approx. 0.25 s, the supply pressure of the hydraulic motor of 40 bar is installed in the hydroaccumulator, acc. to fig. 58.



5.2. Secondary control hydraulic transmission with adjustable capacity pump, variable capacity motor and PID compensator in the speed control loop

In the case of secondary control hydraulic transmissions, including a fixed capacity pump in the primary side and an adjustable capacity motor in the secondary side, substantial energy savings and functional advantages are obtained, if PID (Proportional Integrative Derivative) compensators are used in the hydraulic motor speed control loop.

The energy saving is measurable by the value of the flow rate passing through the pump pressure valve in the primary side of the transmission.

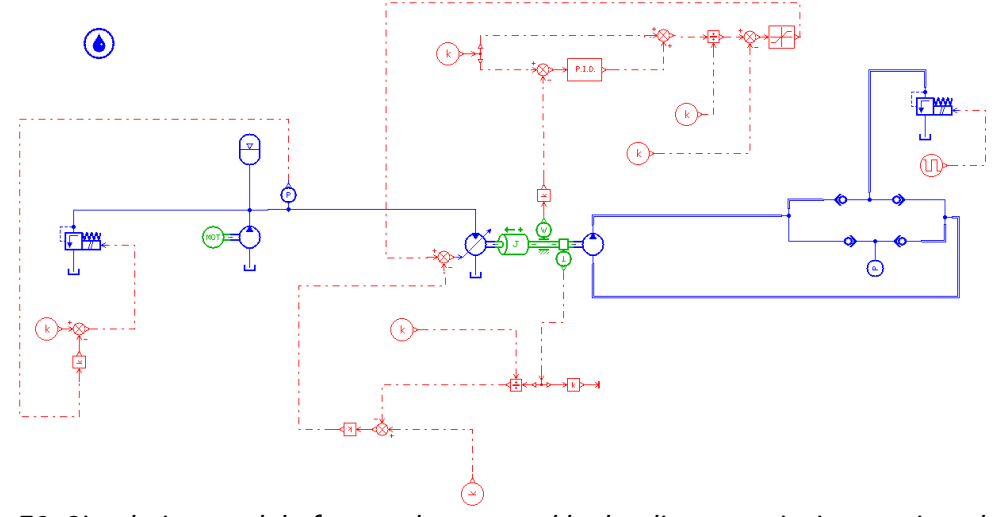


Fig. 59- Simulation model of secondary control hydraulic transmission, equipped with electronic PID type compensator in the speed control loop.

Functional advantages lead to a reduction in the motor speed variation range, depending on the variation of its load, without affecting the dynamic performance regarding the torque developed at the shaft.

The AMESim simulation model, for such a hydraulic transmission with secondary control, is shown in fig. 59, and the results of running this model are shown in fig. 60 ... 65.

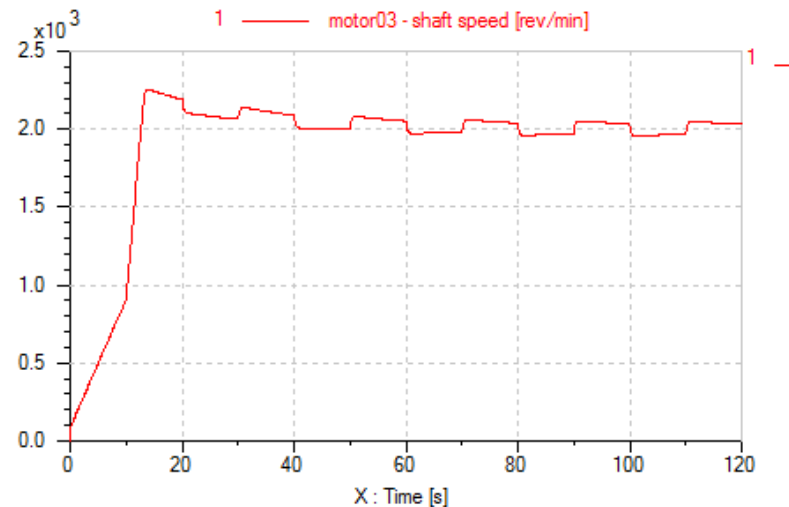


Fig. 60- Variation in the speed rate of hydraulic motor with PID electronic compensator in the speed control loop.



Fig. 60 shows that the speed variation range of the hydraulic motor in the secondary side of the transmission, depending on the variation of its load, stabilizes after 40 s, at a value below 100 rpm.

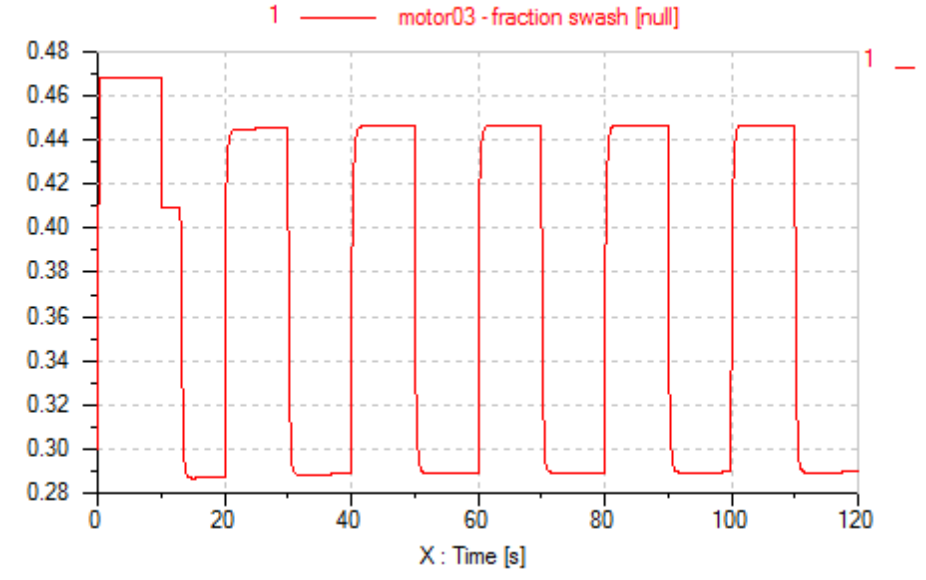


Fig.61- Variation in the capacity of hydraulic motor with PID electronic compensator in the speed control loop.

In order for the variation of the hydraulic motor speed, depending on the variation of its load, to be according to fig. 60, the hydraulic motor automatically adjusts its capacity, according to the curve in fig. 61, to values in the range of 0.47 ... 0.29 of its maximum capacity. The shape of the hydraulic motor capacity variation curve is similar to the rectangular excitation signal of the proportional valve on the discharge circuit of the load pump in the secondary side of the transmission.

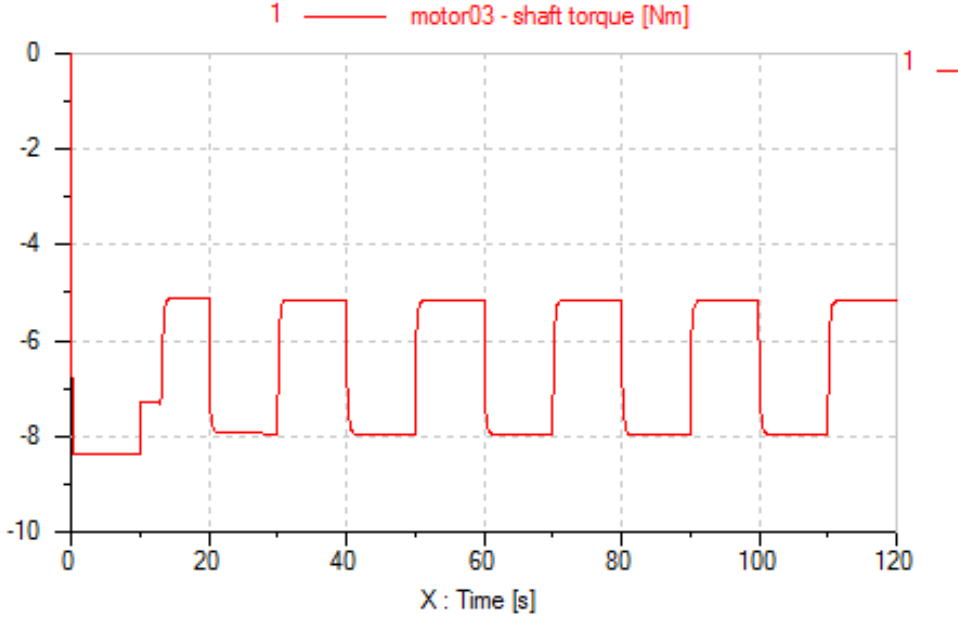


Fig.62- Variation in the torque at the shaft of hydraulic motor with PID electronic compensator in the speed control loop.



During the simulation, the torque at the hydraulic motor shaft varies according to fig.62.

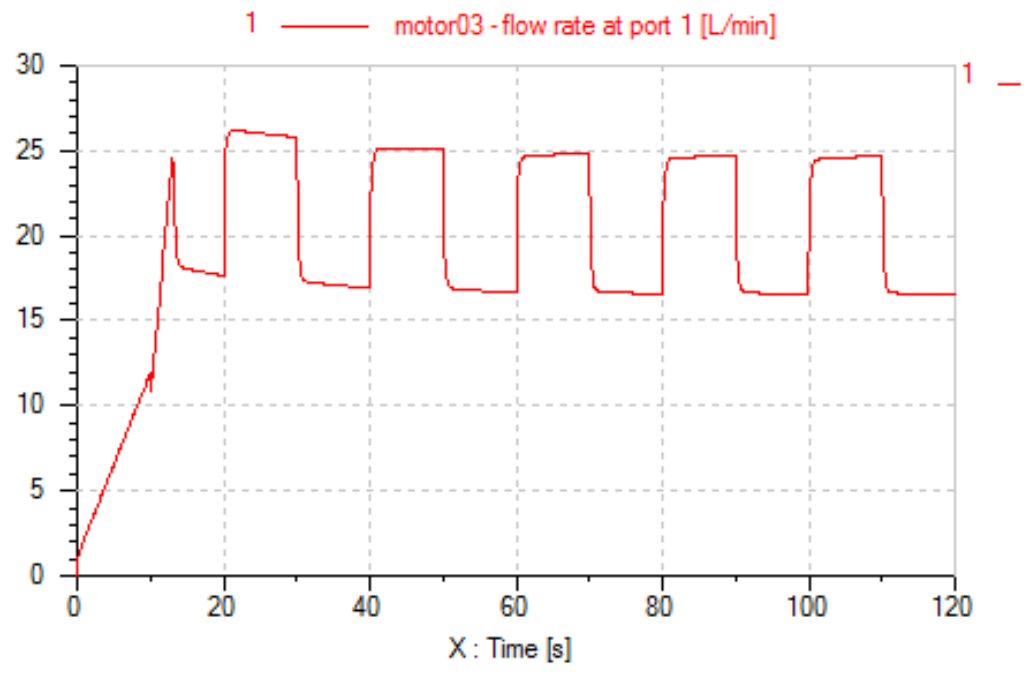


Fig.63- Variation in the flow rate of hydraulic motor with PID electronic compensator in the speed control loop.

In order for the variation in the hydraulic motor torque to be according to fig. 62, the variation curve of flow rate passing through the motor has a shape as in fig. 63.

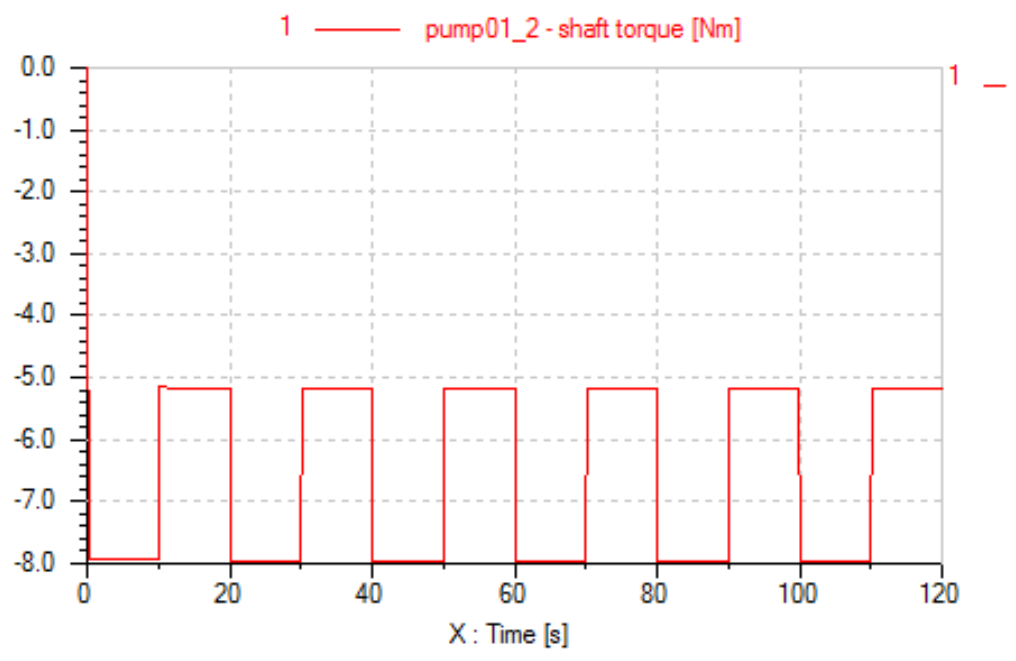


Fig. 64- Variation in the resistance torque at the hydraulic motor shaft.

Variation in the resistance torque at the hydraulic motor shaft, depending on the rectangular excitation signal of the proportional valve on the discharge circuit of the load pump, takes place according to the curve shown in fig. 64.

Throughout the simulation, the supply pressure of the hydraulic motor has a constant value, according to the requirements of the secondary control. In the case of this simulation, the value of the supply pressure of the hydraulic motor is 40 bar, according to fig. 65.

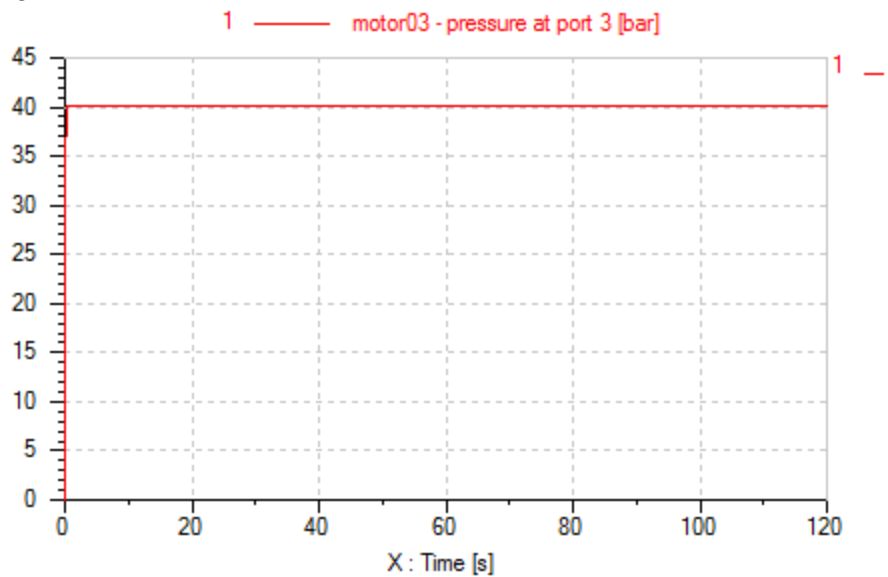


Fig.65- Variation in pressure at the hydraulic motor supply connecting fitting.

5.3. Secondary control hydraulic transmission with adjustable capacity pump, equipped with pressure controller and variable capacity motor

In order to optimize the secondary control hydraulic transmission, from the energy efficiency and functional point of view, the AMESim simulation model of the hydraulic transmission has gone through three stages in succession:

- a) secondary control hydraulic transmission, with fixed capacity pump and variable capacity motor, with P (proportional) type compensator in the speed control loop;
- b) secondary control hydraulic transmission, with fixed capacity pump and variable capacity motor, with PID (proportional, integrative, derivative) type compensator in the speed control loop;
- c) secondary control hydraulic transmission, with adjustable capacity pump equipped with pressure controller and variable capacity motor, with P (proportional) type compensator in the speed control loop.

The following highlights the advantages of the third type of secondary control of hydraulic transmissions. The simulation model of this type of transmission is shown in fig. 66.

The proportional valve on the suction / discharge of the fixed capacity bidirectional load simulation pump has been excited with a rectangular signal, acc. to fig. 67.

The transmission simulation model has been run simultaneously for three distinct values of the maximum capacity of the adjustable motor in the secondary side of the transmission. The three upper values of the motor capacity limitation are given by three preset parameters of the input in the saturation element of the speed controller, namely $0.75\ V_{m.max}$; $0.87\ V_{m.max}$; and $1\ V_{m.max}$, acc. to fig. 68.

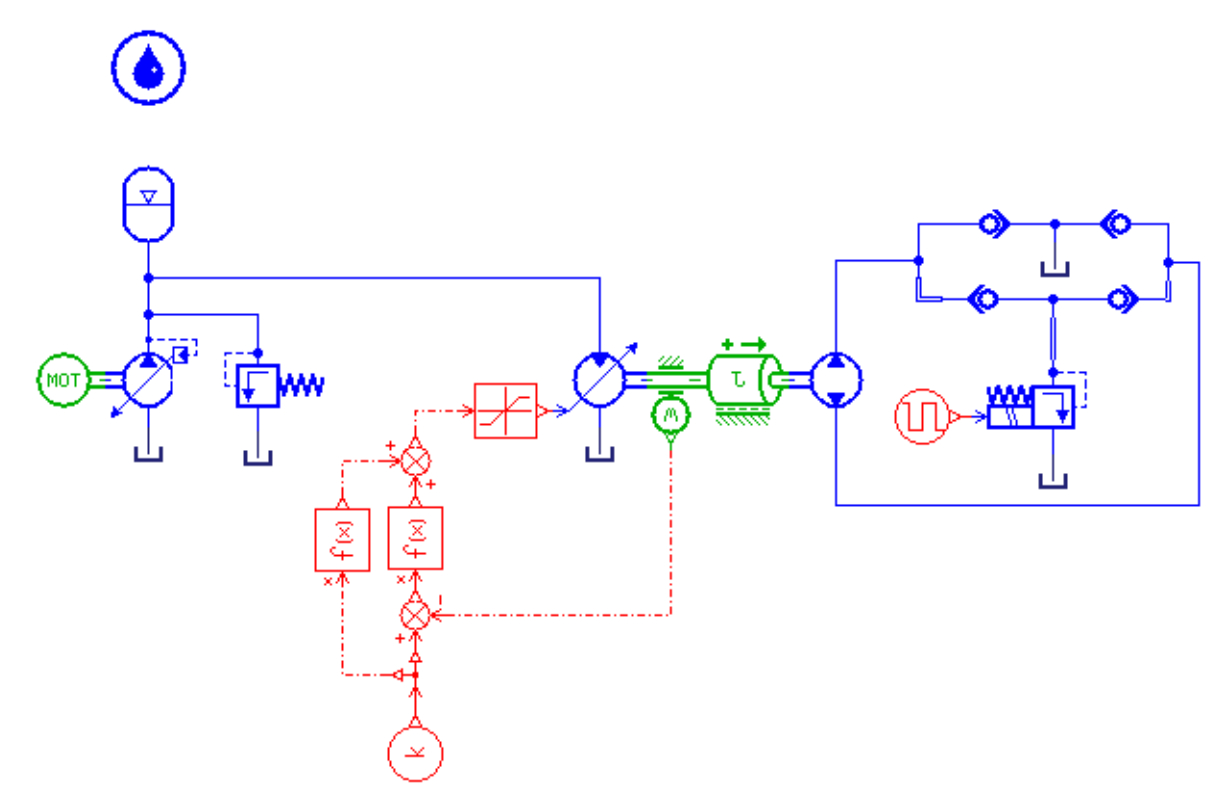


Fig.66- AMESim simulation model of secondary control hydraulic transmission, with adjustable capacity pump in the primary side, equipped with pressure controller.

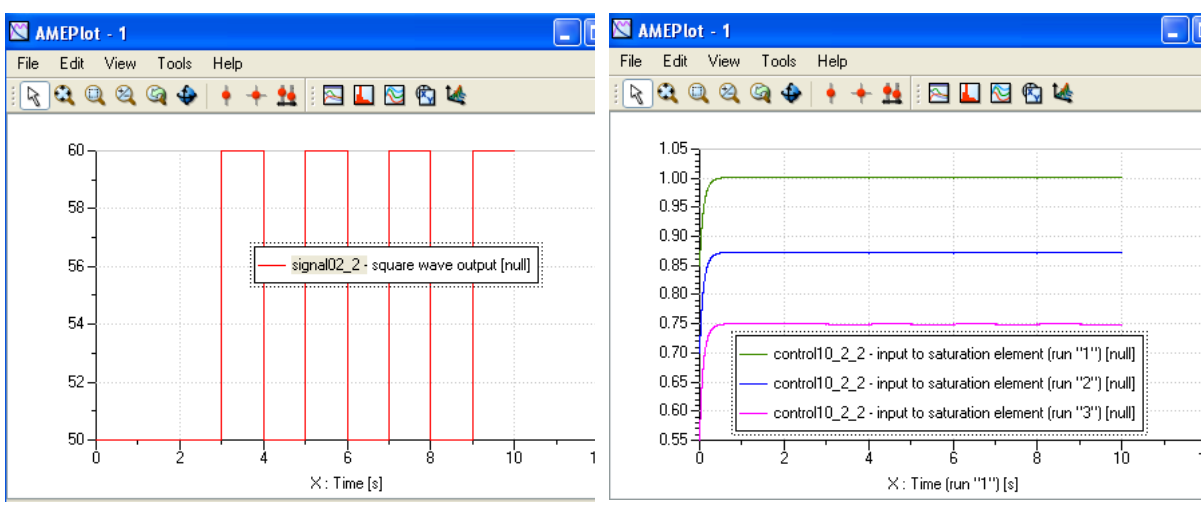


Fig. 67- Rectangular excitation signal of the proportional load simulation valve.

Fig.68- Simultaneous running for three distinct values of the maximum capacity of the hydraulic motor.

From the point of view of the theory of primary and secondary control of hydraulic transmissions, the primary control involves an adjustable capacity pump and a fixed capacity motor, fed at a constant flow rate, while the secondary control involves a fixed capacity pump and an adjustable capacity motor, fed at a constant pressure. From this point of view, the control model addressed is atypical because the motor is fed at a constant flow rate, acc. to fig. 69, and at a variable pressure, acc. to fig. 70.

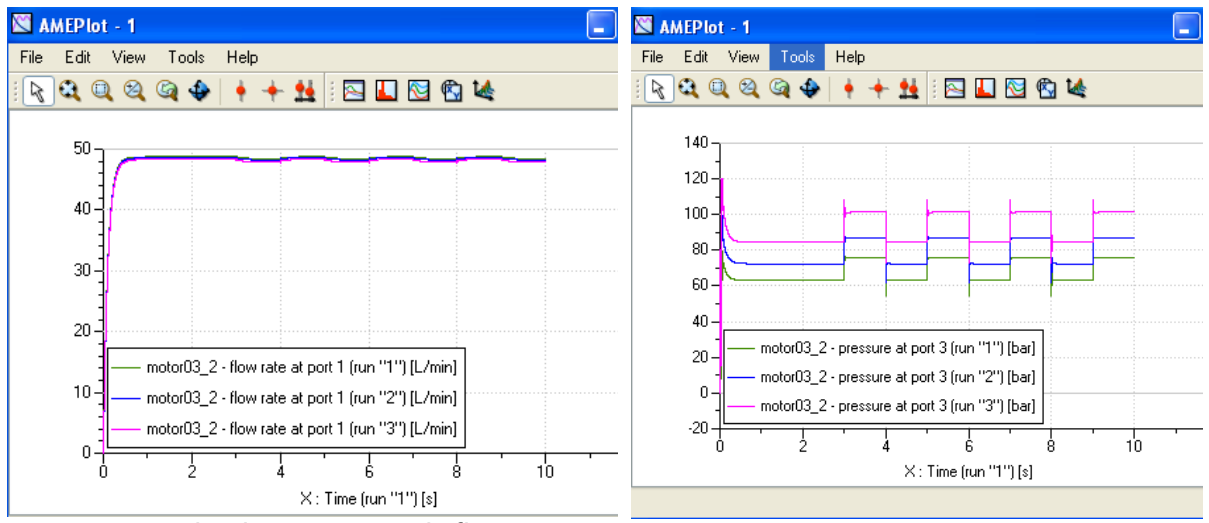


Fig.69- Hydraulic motor supply flow rate variation - 3 simultaneous runs.

Fig. 70- Hydraulic motor inlet pressure variation - 3 simultaneous runs.

As to the type of positive displacement units in the primary and secondary sides, the control model presented contains an adjustable capacity hydraulic motor in the secondary side, according to the theory of secondary control, but the pump in the primary side, equipped with a pressure controller, provides a relatively constant flow rate, regardless of the variation in its outlet pressure due to the load variation of the hydraulic motor in the secondary side.

While there could be controversy regarding the positioning of this type of control in the classification of hydraulic transmission controls - primary, secondary or mixed control - energy and functional benefits cannot be denied.

The energy benefits are demonstrated by the fact that the flow rate passing through the safety valve of the pump in the primary side of the hydraulic transmission is null, acc. to fig. 71, regardless of the torque developed at the hydraulic motor shaft, acc. to fig. 72.

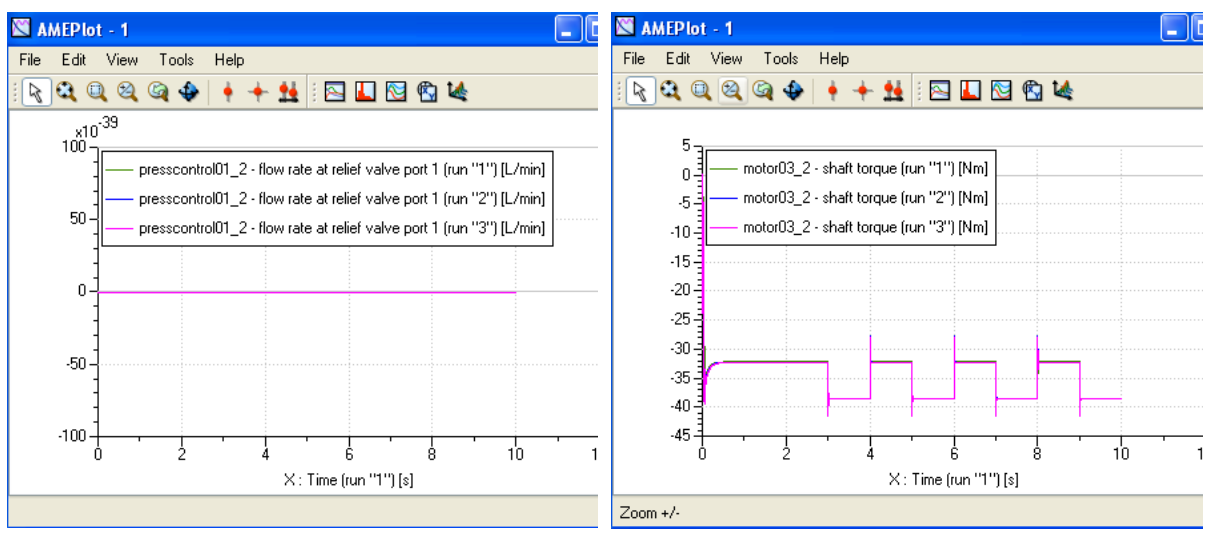


Fig. 71- Variation in the flow rate passing through the pressure valve - 3 simultaneous runs.

Fig.72- Variation in torque at the hydraulic motor shaft - 3 simultaneous runs.



The functional benefits are demonstrated by the fact that the speed variation range of the hydraulic motor, depending on the load variation, is very narrow, acc. to fig. 73.

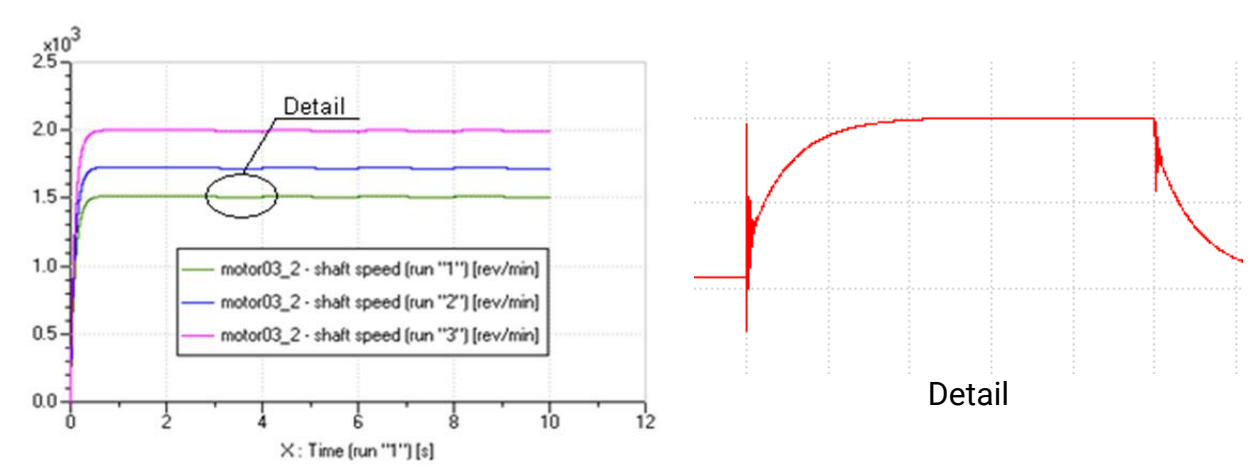


Fig.73- Time evolution of speed in the presence of load disturbances (steps of 125..150 bar in the load simulation circuit) - 3 simultaneous runs.

as well as by the variation of the oil flow rate in the hydraulic accumulator, acc. to fig. 74.

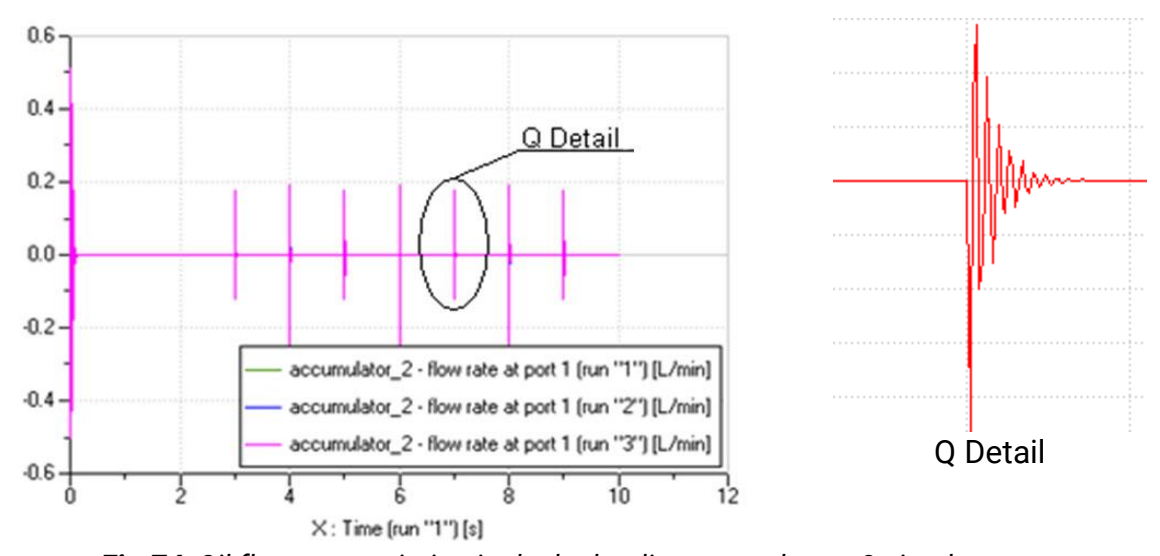


Fig.74- Oil flow rate variation in the hydraulic accumulator - 3 simultaneous runs.

5.4. Conclusions on the secondary control of hydraulic transmissions

- 1. The experimental model of the hydraulic drive system with secondary control comprises all the necessary equipment to highlight its characteristics and performance. The creation of a hydraulic system for the simulation of the resistance load has the advantage that it has a great flexibility in operation and allows a relatively easy change of its functional parameters.
- 2. By numerical simulation, the control possibilities of the drive system, with control algorithms previously developed and implemented in the electronic compensator of the system, have been highlighted.



- 3. The results obtained from numerical simulations allow one to appreciate that the created system offers the possibility to perform complex experiments for the study of various phenomena that may occur in secondary control hydraulic drive systems.
- 4. The energy savings obtained as a result of the use of secondary control systems is highlighted by the value of the flow rate passing through the pressure control valve in the main circuit. To keep the motor speed relatively constant, regardless of the load variation at its output, the capacity of the hydraulic motor is modified, correlated with the value of the supply pressure. This allows the supply pressure to be kept to a minimum so that energy savings are maximized.
- 5. Using a PID electronic compensator in the speed control loop significantly reduces the speed variation range, without affecting the dynamic performance of the torque developed at the shaft.
- 6. For the energy and functional optimization of the secondary control hydraulic transmission, the AMESim simulation model of the hydraulic transmission has gone through three stages in succession:
 - a) secondary control hydraulic transmission, with fixed capacity pump and variable capacity motor, with P (proportional) type compensator in the speed control loop;
 - b) secondary control hydraulic transmission, with fixed capacity pump and variable capacity motor, with PID (proportional, integrative, derivative) type compensator in the speed control loop;
 - c) secondary control hydraulic transmission, with adjustable capacity pump equipped with pressure controller and variable capacity motor, with P (proportional) type compensator in the speed control loop.
- 7. A superior step in optimizing the secondary control of hydraulic transmissions consists in the secondary control hydraulic transmission with adjustable capacity pump, equipped with pressure controller and variable capacity motor, with PID (proportional, integrative, derivative) type compensator in the speed control loop.



BIBLIOGRAPHY

- 1. Vasiliu, N., Catană, I. *Transmisii hidraulice și electrohidraulice*. Vol. I Maşini hidraulice volumice / *Hydraulic and electrohydraulic transmissions*. Vol. I Positive displacement hydraulic machines, Technical Publishing House, Bucharest, 1988.
- 2. Vasiliu, D., Vasiliu, N. Acţionări şi comenzi hidropneumatice în energetică / Hydropneumatic drives and controls in power engineering. (Lithograph). "Politehnica" University of Bucharest, 1993.
- 3. Vasiliu, N., Vasiliu, D. *Acţionări hidraulice şi pneumatice*. Vol. I / *Fluid Power drives*. Vol. I, Technical Publishing House, Bucharest, 2004.
- 4. Popescu, T. C. Cercetări asupra sintezei sistemelor de acţionare hidraulice, / Research on the synthesis of fluid power systems, "Politehnica" University of Bucharest, 2008, Doctoral thesis.
- Popescu, T. C., Blejan, M., Şovăială, Gh. "Experimental research upon accommodating the functional parameters of a laser controlled system designed for a grading machinery with the actual operating conditions of the grading machinery", Proc. SPIE 7297, Advanced Topics in Optoelectronics, Microelectronics, and Nanotechnologies IV, id. 72972D, 2009, doi: 10.1117/12.823697.
- 6. Popescu, T. C., Drumea, A., Duţu, I. "Numerical simulation and experimental identification of the laser controlled modular system purposefully created for equipping the terrace leveling installations", *Proc. of 2008 31st International Spring Seminar on Electronics Technology*, pp. 334-339, 2008, doi: 10.1109/ISSE.2008.5276663.
- 7. Blejan, M., Lupu, B., Duţu, I., Rotaru, D., Popescu, T. C. "Electronic oscillator for a hydraulic flow divider", *Proc. of 2009 32nd International Spring Seminar on Electronics Technology*, 2009, Poster Session (E), E01, pp. 1-3, doi: 10.1109/ISSE.2009.5207014.
- 8. Popescu, T. C., Duţu, I., Vasiliu, C., Mitroi, M. "Adjustment of conformity parameters of PID-type regulators using simulation by AMESim", *Proc. of 7th International Industrial Simulation Conference ISC 2009*, Article no. ENERG_01, pp. 269-274, 2009.
- 9. Popescu, T. C., Ion Guţă, D. D., Marin, Al. "Adjustment of hydrostatic transmissions through virtual instrumentation technique", *Proc. of 8th International Industrial Simulation Conference ISC 2010*, Article no. ENERG_02, pp. 248-253, 2010.
- 10. Popescu, T. C., Drumea, P., Ion Guţă, D. D. "Research activities regarding energetic and functional advantages of hydraulic transmissions", *Proc. of 10th International Multidisciplinary Scientific Geo-Conference & Expo SGEM 2010*, Vol. 2, pp. 323-330, 2010.
- 11. Ion Guță, D. D., Popescu, T. C., Dumitrescu, C. "Optimization of hydrostatic transmissions by means of virtual instrumentation technique", *Proc. SPIE 7821, Advanced Topics in Optoelectronics, Microelectronics, and Nanotechnologies V* id. 782129, 2010, doi: 10.1117/12.881904.